Manuscript prepared for Atmos. Chem. Phys.
with version 3.2 of the LaTeX class copernicus.cls.
Date: 14 April 2015

Evaluation of updated nitric acid chemistry on ozone precursors and radiative effects

K.M. Seltzer[1], W. Vizuete[2], and B.H. Henderson[1]

[1]Department of Environmental Engineering Sciences, University of Florida, Gainesville, FL, USA
[2]Department of Environmental Science and Engineering, University of North Carolina, Chapel Hill, NC, USA

Correspondence to: K.M. Seltzer (karlseltzer@gmail.com), B.H. Henderson (barronh@ufl.edu)

Abstract. This study shows that revising the reaction rate of $NO_2 + HO^{\cdot} \longrightarrow HNO_3$ improves simulated nitrogen partitioning and [..[1]]changes the simulated radiative effects of several [..[2]]short-lived climate forcers (SLCF). Both laboratory and field study analysis have found that the reaction rate should be reduced by 13-30% from current recommendations. We evaluate the GEOS-Chem model over North America with and without the recommended update using observations from the INTEX-NA Phase A campaign. Revising the $NO_2 + HO^{\cdot} \longrightarrow HNO_3$ rate coefficient improves model performance of oxidized nitrogen partitioning by increasing NO_x concentrations in the upper troposphere and decreasing HNO_3 throughout the troposphere. The [..[3]][..[4]]increase in NO_x [..[5]]concentrations has a corresponding global increase in O_3 concentrations and [..[6]]local increases in sulfate aerosols, causing a perturbation in the simulated radiative effects of tropospheric ozone. These findings demonstrate the [..[7]]positive influence the mechanism update has on the [..[8]]partitioning of oxidized nitrogen species, the benefits it provides when compared to aircraft observations and the simulated radiative effects that the reduction induces.

1 INTRODUCTION

Global chemical transport models (GCTMs) are excellent tools for exploring our scientific understanding. They are used to estimate concentrations fields, develop source/sink budgets for compounds, source/receptor relationships, infer emission inventories, and estimate the impact of emission reduction strategies (e.g., Jaegl et al., 2003; Fusco and Logan, 2003; West et al., 2006; Chen et al., 2009; Millet et al., 2010; West et al., 2009; Kopacz et al.,

[1]removed: adjusts
[2]removed: radiative forcing variables
[3]removed: downward revision of the
[4]removed: rate increases the lifetime of
[5]removed: , increases
[6]removed: increases
[7]removed: influence the rate revision
[8]removed: composition of the atmosphere

2010). The benefit of [..[9]]GCTM's to their regional counterparts is the scale that decreases sensitivity to boundary conditions [..[10]](Jacobson, 2005). When new information on a process emerges in the literature, the GCTM must be evaluated in the context of that [..[11]]update. In addition, an understanding into how this update would have influenced conclusions from previous studies must be considered.

GCTMs are often used to predict [..[12]]ozone and aerosol concentrations that are products of photochemical oxidation. In the context of oxidation, the chemical component of GCTMs (a.k.a. chemical mechanism) indirectly influences all the other processes. Chemical transformation directly changes the chemical availability of compounds and the physical properties of compound families. For instance, [..[13]]Reaction 1 decreases the photochemical availability of a hydroxyl radical ($HO^{\cdot}$) and nitrogen oxides ($NO_x = NO + NO_2$). Reaction 1 also increases the solubility of oxidized nitrogen [..[14]]since the Henry's Law coefficient for HNO_3 (2.1×10^5 M/atm at 298 K) is seven orders of magnitude greater than that of NO_2 (10^{-2} M/atm at 298 K). Uncertainty in [..[15]]Reaction 1 would, therefore, affect the lifetime of NO_x emissions and the lifetime of NO_y as a NO_x reservoir. This is [..[16]]important for other molecules such as ozone since ozone production is limited, on average, by NO_x availability (Sillman et al., 1990; McKeen et al., 1991; Chameides et al., 1992; Jacob et al., 1993; Jaegl et al., 1998a).

$$NO_2 + HO^{\cdot} \longrightarrow HNO_3 \tag{1}$$

Reaction 1 is widely recognized as a key reaction in atmospheric oxidation (e.g., Seinfeld, 1989; Donahue, 2011), but has not been well constrained. Despite its known influence [..[17]]and importance, Reaction 1 has [..[18]]proven difficult to measure at temperatures and pressures in the troposphere (Donahue, 2011). In a recent study, Mollner et al. (2010) employed state-of-the-science techniques to accurately measure the reaction rate at standard temperature and pressure ($T = 298\mathrm{K}$ and $P = 1\mathrm{atm}$). In a subsequent study, Henderson et al. (2012) constrain the rate of [..[19]]Reaction 1 using aircraft measurements from the upper troposphere ($T = 240\mathrm{K}$ and $P = 0.29\mathrm{atm}$). Both of [..[20]]these studies recommend significant downward revisions[..[21]], and the rate recommended in the upper troposphere suggests an update to the temperature sensitivity (Henderson et al., 2012). [..[22]]As will be demonstrated in this study, updates to the rate of [..[23]]Reaction 1 have the potential to

[9] removed: GCTMs
[10] removed: . The trade off is increased sensitivity to modeled processes including emissions, transport, and chemistry. The uncertainty in processes can have competing effects that make them difficult to identify even when the uncertainty influences the research subject.
[11] removed: new information. We must also understand how updating a process
[12] removed: or estimate the ozone and aerosols
[13] removed: reaction
[14] removed: because
[15] removed: reaction
[16] removed: particularly important to ozone in its climate forcing capacity because, on average,
[17] removed: , reaction
[18] removed: proved
[19] removed: reaction
[20] removed: the studies above
[21] removed: of the rate
[22] removed: Updates
[23] removed: reaction

change NO_x[..[24]], radical, and ozone concentrations. As well, since tropospheric ozone [..[25]]is a short-lived climate forcer (SLCF), changes in the [..[26]]simulated radiative flux is expected. This study implements the [..[27]]mechanism update in the GEOS-Chem chemical transport model and evaluates the [..[28]]impacts related to oxidized nitrogen partitioning. In addition to the effects on oxidized nitrogen partitioning and ozone precursors, the study also utilizes an offline radiative transfer model to evaluate the [..[29]]simulated instantaneous radiative forcing that this mechanism update produces. We hypothesize that the increased NO_x lifetime will increase NO_x concentrations, decrease HNO_3 concentrations, reduce the ratio of $HO_2^{\cdot}$ to $HO^{\cdot}$ concentrations, [..[30]][..[31]]and lead to localized positive radiative effects [..[32]]where ozone increases occur.

2 METHODS

[..[33]][..[34]][..[35]][..[36]][..[37]][..[38]]

Model Description

We simulate the INTEX-NA, Phase A (INTEX-A) time period (July - August 2004) using the GEOS-Chem global chemical transport model (version 9-01-02; http://www.as.harvard.edu/chemistry/trop/geos/). The GEOS-Chem model explicitly simulates tracer species advection, diffusion, deposition, gas-phase reactions, and equilibrium partitioning of [..[39]]gasses and aerosols. This is accomplished by using inputs for meteorology, emissions, and chemistry[..[40]]. We configured GEOS-Chem to [..[41]]simulate July 1st to August 30th[..[42]], with chemical concentrations produced at a horizontal resolution of 2° by 2.5° and 47 vertical levels. We evaluated levels 1 through 32, which range in resolution from 120 m near the surface to 1000 m at the top of the model. The simulated time frame covers the period observed by the National Aeronautics and Space Administration (NASA) aircraft (DC-8). [..[43]]While we have simulated global fields, the model evaluation [..[44]]covers the Northern Hemisphere, primarily over North America (see Figure 1). The meteorological inputs are produced by the NASA Global Modeling and Assimilation Office (GMAO) and assimilate observations from the Goddard

[24] removed: concentrations, radicalconcentrations, ozone concentrations and sensitivity to emission reduction strategies (Cohan et al., 2010)
[25] removed: has strong influences on the radiative budget of the atmosphere
[26] removed: atmospheric radiation balance predicted by GCTMs will occur
[27] removed: updated rates
[28] removed: impact
[29] removed: predicted direct radiative forcing (DRF) changes
[30] removed: increase ozone sensitivity to
[31] removed: emission reductions,
[32] removed: in locations
[33] removed: In this study, we evaluate the influence the updated chemical mechanism has on model estimates of trace gas composition in the troposphere and radiative effects on the surface and effective top of atmosphere. The base model will be described in the
[34] removed: section and the chemistry updates in the
[35] removed: section. The observations and their associated uncertainty are described in the
[36] removed: section. The method of evaluation used to incorporate measurement uncertainty is described in the
[37] removed: section. The methods used to determine the radiative effets of the chemical mechanism update are discussed in the
[38] removed: section.
[39] removed: gas to aerosol
[40] removed: inputs to produce predictions concentration fields
[41] removed: produce concentration fields from
[42] removed: . The concentration fields are produced at
[43] removed: Although
[44] removed: will cover

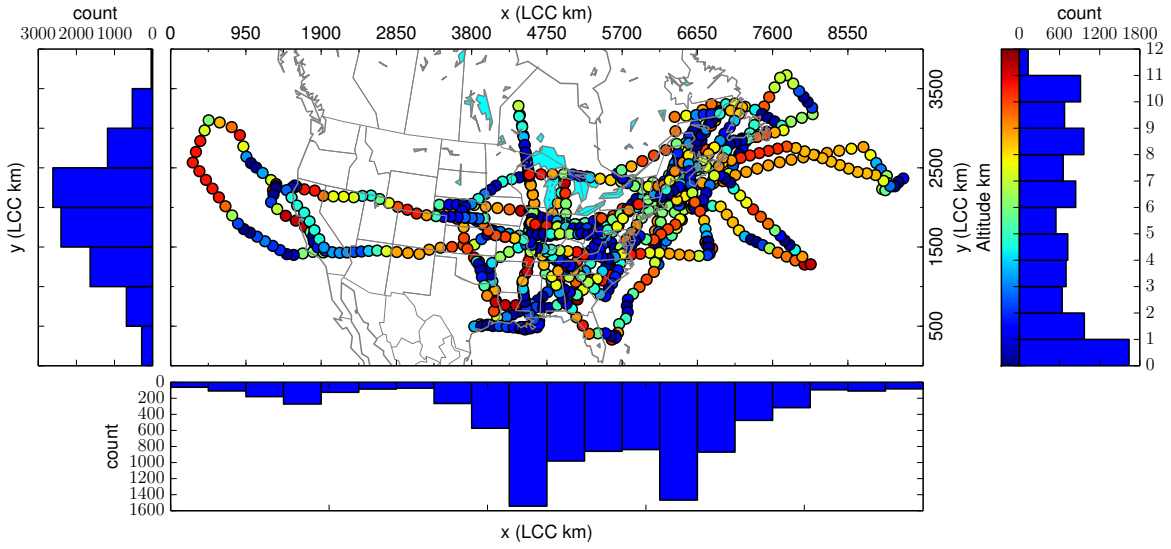

Fig. 1. Sample locations (dots) from the INTEX-A campaign with altitude shown in color with histograms for latitude and longitude. The dots show every tenth sample, but the histograms use all samples.

Earth Observing System version 5 (GEOS-5). The GEOS-5 system is the latest version and has observations starting on January 1 of 2004. The model was configured to use cloud convection with a 15-minute [..[45]]time step and planetary boundary mixing with the non-local option. The emissions include biomass (van der Werf et al., 2006), biogenic (Guenther et al., 2006), lightning (Ott et al., 2010), and anthropogenic emissions (described below).

Anthropogenic emissions of NO_x, CO, and SO_2 are included at both a global and regional scale. At the regional scale, anthropogenic emissions of NO_x, CO, and SO_2 are specifically provided for the United States of America, Europe, Mexico and South-East Asia. The United States emissions are derived from the EPA's National Emission Inventory (NEI) for the year 2005 and supplemented by the biofuel emission inventory from 1999. In contrast to the 1999 NEI, the mobile NO_x emissions from the [..[46]]2005 NEI have compared well to fuel use estimates (Parrish, 2006; Dallmann and Harley, 2010). The European emissions are provided by the Co-operative Programme for Monitoring and Evaluation of the Long-range Transmission of Air Pollutants in Europe (EMEP) inventory for Europe in 2000 by Vestreng and Klein (2002). The Mexico emissions are derived from the 1999 Big Bend Regional Aerosol and Visibility Observational (BRAVO) emissions inventory for Mexico (Kuhns et al., 2003). [..[47]]Asia emissions are derived from Streets et al. (2003, 2006). For the rest of the world, emissions are [..[48]]derived from the EDGAR fossil fuel inventory and scaled from the year 2000 (Olivier et al., 2002).

Chemistry Updates

In this study, we compare simulations with standard chemistry (base case) and revised chemistry (HNO3 case). The reaction rate of $NO_2 + HO^{\cdot}$ is decreased to account for emerging literature recommending a downward re-

[45] removed: timestep
[46] removed: 2000
[47] removed: The
[48] removed: included

vision (Mollner et al., 2010; Henderson et al., 2012). [..[49]]Mollner et al. (2010) recommend a 13% [..[50]]decrease to the rate recommended by Sander et al. (2011), which is lower than that recommended by Atkinson et al. (2004). Donahue (2011) commended the recent work by Mollner et al. (2010), but asserted that there is remaining uncertainty. Henderson et al. (2012) also re-evaluated the rate constant using Bayesian inference and measurements from the upper troposphere. The evaluation in the upper troposphere complements the Mollner et al. (2010) study with information at temperatures from 230-250 K. Henderson et al. (2012) conclude that the temperature sensitivity is currently overestimated and should be revised according to Equations 2 and 3. As such, updates to GEOS-Chem in the HNO3 case are as follows:

$$k_0 = 1.49 \times 10^{-30} \left(\frac{T}{300}\right) [..^{51}]^{-1.8} \quad (2)$$

$$k_\infty = 2.58 \times 10^{-11} \quad (3)$$

[..[52]]Observation Description

In this study, we evaluate the model [..[53]]using aircraft observations from the INTEX-A campaign. The INTEX-A campaign collected observations from 90 m to 11.9 km covering North America [..[54]](Fig. 1). The suite of measurements [..[55]]from this campaign included inorganic species (NO, NO_2, PAN, HNO_4, HNO_3, O_3, H_2O_2 and CO) and organic species (CH_2O, CH_3CHO, and $CH_3C(O)CH_3$). As with other studies (e.g., Hudman et al., 2007), the observations are filtered to exclude stratospheric intrusion, biomass burning, wildfires, and fresh pollution plumes. These events are excluded because the model is not designed to capture the variability of extreme events, or events on a horizontal scale smaller than the model resolution. First, [..[56]]stratospheric intrusion is identified when the ratio of O_3 to CO is greater than 1.25. Biomass burning is identified by [..[57]]concentrations of hydrogen cyanide and acetonitrile greater than 500 ppt [..[58]]and 225 ppt, respectively. Fresh pollution plumes are identified where NO_x was more than 40% of the total oxidized nitrogen ($NO_y \equiv NO_x + PAN + HNO_3$), or if NO_y is not available, when $NO_2 > 400$ppt and below 3 km. [..[59]][..[60]][..[61]]

For each measurement, an estimation or calculation of the uncertainty [..[62]]in the measurement technique was carried out. Depending on the measurement, the uncertainty was either provided [..[63]]on a per-sample basis or for the whole dataset. Absolute uncertainty is provided on a per sample basis, while relative uncertainty is provided for the dataset. Relative uncertainty (1σ) was provided for O_3 ($\pm 5\%$), $HO^{\cdot}$ ($\pm 15\%$), $HO_2^{\cdot}$ ($\pm 15\%$),

[49] removed: The recommendation by Mollner et al. (2010) is
[50] removed: below
[52] removed: Observations
[53] removed: with respect to
[54] removed: .
[55] removed: includes inorganic species
[56] removed: plumes that are identified in the flight logs were removed. Then biomass
[57] removed: hydrogen cyanide
[58] removed: or acetonitrile greater than
[59] removed: Stratospheric intrusion is identified when the ratio of
[60] removed: to
[61] removed: is greater than 1.25.
[62] removed: of
[63] removed: for the whole dataset or

PAN ($\pm 15\%$), and NO_2 ($\pm 5\%$). For HNO_3 (measured by P. Wennberg at the California Institute of Technology), uncertainty was provided as a column-wise absolute uncertainty that combines calibration, water correction [..[64]]and background signal. The uncertainty was propagated from the 0.5 s time-scale to the 1 min time-scale through linear propagation[..[65]]. The HNO_3 relative error simple average is 20%, median is 12%, 75^{th} percentile is 19% [..[66]]and the concentration weighed average is 11%.

[..[67]]The NO_2 measurement [..[68]]has a known interference at low temperatures (Browne et al., 2011). At low ambient temperatures, pernitric acid (HNO_4) and methyl peroxy nitrate ($CH_3O_2NO_2$; MPN) dissociate in the inlet tube, adding molecules of NO_2 to the measurement. When temperatures are above 255 K , the interference is less than 5% and within stated uncertainty limits (Browne et al., 2011). [..[69]]However, when temperatures are below 255 K, [..[70]]such as in the upper troposphere, the interference can be more than 15%. [..[71]]For temperatures below 255 K, we use a chemical box-model (Henderson et al., 2012) to estimate the concentration of MPN and reduce the NO_2 measurement accordingly. This chemical box model was validated with a modified version of GEOS-Chem that included MPN (not shown). Post-analysis of [..[72]][..[73]]MPN suggests that the difference between the two models was less than a factor of two. Box-model median [..[74]]MPN concentrations were 14 ppt at 8 km and 17 ppt at 10 km. The modified GEOS-Chem [..[75]][..[76]]median MPN concentrations were 15 ppt from 8 to 9 km and 34 ppt from 9 to 10 km. Above 10 km, the uncertainty in our box model MPN predictions increase, which leads us to evaluate the mechanism update only below 10 km. Although there are differences between the two models below 10 km, they are insufficient in magnitude to alter our conclusions. In addition to individual measurements, this analysis focuses on species groups and algebraic combinations of measurements. The two most notable species groups are NO_x ($NO + NO_2$) and NO_y ($NO_x + PAN + HNO_3$) and their uncertainty is simply the root of the summed squared error for each group.

For nitric oxide (NO), the direct measurement is not sensitive at the concentrations studied here. Nitric oxide [..[77]][..[78]]was measured by chemiluminescence with a 50 ppt lower-limit of detection, which is too high to characterize the middle free troposphere (e.g., Bertram et al., 2007; Singh et al., 2007). As a result, we calculate steady-state NO as described in Eq. 4, where j is the photolysis rate, T is [..[79]]the temperature and "[]" denote concentrations. The uncertainty in the derived NO value is propagated from NO_2, O_3, and HO_2, with the assumption that temperatures and reaction rates are precisely known.

[64] removed: ,
[65] removed: ($\sigma = \sqrt{n^{-1}\sum_i^n \sigma^2}$)
[66] removed: ,
[67] removed: For the
[68] removed: , the measurement
[69] removed: When
[70] removed: the
[71] removed: Below
[72] removed: suggests that this approach provided
[73] removed: concentrations within
[74] removed: concentrations predicted
[75] removed: model
[76] removed: predictions are between
[77] removed: (
[78] removed:)
[79] removed: temperature,

Table 1. Measurement descriptive statistics (mean: $\overline{X}$, percentiles: 5%, 50%, 90%), average relative uncertainty as a percent $\overline{\left(\frac{\sigma_x}{X}\right)}\%$, and absolute uncertainty in measurement units.

Measured (unit)	N	$\overline{X}$	5%	50%	95%	$\overline{\left(\frac{\sigma_x}{X}\right)}\%$	$\overline{\sigma}$
NO	3745	95.1	4.9	30.1	361.9	7.3	6.9
NO_2	3995	94.9	7.8	39.8	335.4	5.0	4.7
HNO_4	2399	37.5	1.5	24.2	111.4	23.0	8.6
PAN	3046	268.9	13.0	225.8	658.4	15.0	40.3
HNO_3	2423	420.6	59.8	313.2	1109.8	21.0	51.1
NO_x	3745	182.1	14.3	77.4	621.7	4.7	9.0
NO_z=PAN+HNO_3	1818	680.2	165.7	569.6	1527.8	12.2	68.3
NO_y=NO_x+PAN+HNO_3	1743	819.0	208.4	668.4	1919.1	9.9	68.3

$$[\mathrm{NO}]_{ss} = \frac{j[\mathrm{NO_2}]}{3.3\times10^{-12}\times\exp\left(\frac{270}{T}\right)[\mathrm{HO_2}] + 3.0\times10^{-12}\times\exp\left(\frac{-1500}{T}\right)[\mathrm{O_3}]} \quad (4)$$

[..[80]][..[81]][..[82]][..[83]][..[84]]

Descriptive statistics and uncertainties for the INTEX-A measurements are characterized in Table 1. The table summarizes uncertainty evaluated for the whole dataset, but the uncertainty at each altitude varies. For each measurement, Table 1 shows the number of valid measurements, mean ($\overline{X}$), percentiles (5%, 50%, and 75%), and mean uncertainties (relative $\overline{\left(\frac{\sigma_x}{X}\right)}\%$; absolute [..[85]]$\overline{\sigma}$ in measurement units).

Method of Model Evaluation

The simulations [..[86]]spatially average concentration over a 48,000 km^2 area, [..[87]]reducing the variance of chemical [..[88]]concentrations. While the observations also spatially average [..[89]]concentrations, their line segments only range from 4 to 17 km. Based on these differences alone, we expect the observed and simulated [..[90]]population datasets to each have their own mean and variance for each chemical species. [..[91]]For log-normally distributed species ([..[92]]NO_x, HNO_3)[..[93]], the means cannot be compared because the variances are expected to be different. In this case, the species can be log-transformed to reduce the bias of the mean, but the variances of the observations and model are still different. [..[94]]This difference precludes certain statistical

[80] removed: In addition to individual measurements, this analysis focuses on species groups and algebraic combinations of measurements. The two most notable species groups are
[81] removed: (
[82] removed:) and
[83] removed: (
[84] removed:). The uncertainty for species groups is simply the root of the summed squared error.
[85] removed: $\overline{\sigma_x}$
[86] removed: described above have inherent uncertainty and must be evaluated using observations that also have uncertainty. The simulations
[87] removed: which can reduce
[88] removed: species by averaging highs and lows. The
[89] removed: , but only over line segments that
[90] removed: set will each have its
[91] removed: The mean concentration for a
[92] removed: e.g.,
[93] removed: is highly sensitive to the variance of the results. For log-normally distributed species
[94] removed: The difference in variances

evaluation techniques[..[95]]

[..[96]], such as the Student's t-test[..[97]], from being used in this evaluation.

The alleviate this problem, a variant of the Student's t-test[..[98]], called the Welch's t-test[..[99]], is used. The Welch's t-test (hereafter t-test) is a variant of the Student's t-test that calculates the combined variance using the Welch-Satterthwaite equation (Welch, 1947). [..[100]]The t-test estimates the probability that the measured and modeled mean could be obtained given repeated sampling, with the assumption that the true means are the same. This type of test does not inherently account for potential bias in the measurements, but can be used as part of a framework that does.

[..[101]]The true bias of a measurement cannot be known until it is compared to a superior method under similar circumstances. There is, currently, insufficient data to fully characterize all the biases of measurements made during the INTEX-A campaign. For some measurements, however, multiple techniques produce different answers or subsequent analysis demonstrates a bias. [..[102]][..[103]][..[104]][..[105]]

In order to account for measurement uncertainty, we use a method referred to as the two one-sided t-tests (TOST) (Schuirmann, 1987). Using TOST, we can test whether the model predictions are within measurement uncertainty by rejecting one of two null hypotheses. The first null hypothesis is that the simulated mean is greater than the observations adjusted to their lower bound. The second null hypothesis is that the simulated mean is less than the observations adjusted to their upper bound. If we reject either hypothesis, we have rejected that the model mean is equivalent to the [..[106]]observation mean. This approach is equivalent to assuming a systematic bias equal to the uncertainty in the measurement.

Using relative uncertainty, we formulate the null hypotheses ($H_{0,1}$ and $H_{0,2}$, shown below) using products. For each measurement, the observed accuracy is based on an estimate, which can be found in the header of the observation files. [..[107]]

$$H_{0,1} : \mu_{mod} \geq \mu_{obs \times (1-U)}$$

$$H[..[108]][..[109]]_{0,2} \mu_{mod} \leq \mu_{obs \times (1+U)}[..[110]]$$

[..[111]]

[95] removed: .

[96] removed: We account for different variances and observational uncertainty using a variant of

[97] removed: . The

[98] removed: assumes that the variances of the two populations are identical. The variances are not expected to be identical and, therefore, the standard Student

[99] removed: is not appropriate for this evaluation

[100] removed: Although the t-test can now compare the measurements and predictions, it cannot yet account for measurement accuracy.

[101] removed: Having accounted for the variances, we must now address the reported accuracy and precision tolerances of the observations.

[102] removed: For example, we now know that the

[103] removed: measurement has an interference from peroxy nitrates. The methyl peroxy nitrate interference ranges from 2.5% at 265

[104] removed: to 60% at 225

[105] removed: . Therefore, we need to estimate measurement accuracy and account for it in our evaluation technique.

[106] removed: observations

[107] removed: An alternative formulation is to produce a confidence interval for the difference and compare that to the uncertainty of the mean. We did not use this approach because it does not account for adjustments to observational variance when uncertainty is provided as a factor.

[111] removed: The null hypotheses are formulated to give the benefit of doubt to the model. The joint null hypothesis is that the model is within uncertainty, which must be rejected to conclude that the model is different (greater or less than) from observations. A higher bar would

For each simulation, we evaluate the model in 1 km vertical [..[112]]bins. This method of evaluation was chosen since temperature, pressure, and transport [..[113]]have large variability throughout the vertical troposphere, and these variables play a strong role in the rate of [..[114]][..[115]]

[..[116]]Reaction 1. In each vertical bin, we compare populations of observed and simulated chemical concentrations. By default, the plane flight sampling in GEOS-Chem outputs one prediction for each observation. [..[117]]The model's larger spatial and temporal averaging, however, means that a model grid cell can be paired with more than one observation. In [..[118]]these occurrences, model predictions were not double counted. Following this process, two datasets (observations and predictions) [..[119]]existed for each altitude bin that combined to represent a sample of the atmosphere.

[..[120]]

[..[121]]

[..[122]]

We evaluate the model by using the t-test for species and species groups [..[123]]to examine their bias. This evaluation will include [..[124]]NO_x [..[125]][..[126]]and the family of compounds involved in [..[127]]its cycling, which largely drives photochemical ozone production. As such, we evaluate NO_x and its products by defining NO_y as the sum of NO_x, PAN, and HNO_3 ($\frac{NO_x+PAN+HNO_3}{NO_x+PAN+HNO_3+HNO_4+RNO_3} > 88\%$ for 90% of all samples). [..[128]]Since there is a bias in NO_y (see Results), [..[129]]the evaluation of NO_y components is performed on a normalized basis.

be equivalence testing where we reverse the null and alternative hypotheses. As defined, the analysis is conservative with respect to model evaluation.

[112]removed: divisions to capture the influence of

[113]removed: . Temperature and pressure affect

[114]removed: chemical reactions including the reactions that produce

[115]removed: . The affect of temperature/pressure sensitivity can, therefore, only be seen by evaluating the model with respect to altitude.

[116]removed: When using statistical tests like the t-test, we must be careful to maintain the independent and identically distributed assumption

[117]removed: These pairs help to preserve identical distribution because observations and predictions will represent the same geographic regions.

[118]removed: this case, the set of model predictions will contain duplicates that must be removed to maintain independence. After removing duplicates, we have

[119]removed: that are each a representative

[120]removed: For each altitude, we compare the observed and simulated values of chemical concentrations. To reduce the influence of spatial averaging on variance, variables that demonstrate log-normal distributions will be log-transformed. By log transforming, the distribution becomes symmetric and reduces the skews influence on the mean. By converting all variables to normal distributions, we also allow for the use of statistical tests like the t-test.

[121]removed: When equivalence of observations and simulations is rejected, we examine the bias further. For bias calculations, the duplicate model results are not removed. By retaining duplications, each observation can be paired with a prediction. This allows us to calculate the mean normalized bias ($\overline{B}_N$) as defined in Equation **??**. In Equation **??**, o_i is an observation, y_i is a prediction, and n is the number of pairs. The number of pairs varies by compound because some observations are more available than others.

[123]removed: and examining

[124]removed: the

[125]removed: cycling that drives photochemical ozone production. For

[126]removed: , it is important to evaluate

[127]removed: it's cycling

[128]removed: Because

[129]removed: we also evaluate its components as a fraction of the total

Radiative Effects

Changes in nitric acid formation affect the concentrations of various [..[130]]SLCF. These forcers have the capacity to affect localized climate and change the radiative budget. For this study, these forcings are largely driven by [..[131]]changes in tropospheric ozone concentrations[..[132]][..[133]]

. To assess the radiative effects of changing the nitric acid reaction rate, the Parallel Offline Radiative Transfer (PORT) model was [..[134]]used (Conley et al., 2013). This standalone model was developed at the National Center for Atmospheric Research (NCAR) and isolates the radiation code from the Community Atmosphere Model (CAM). [..[135]]The model calculated the direct instantaneous radiative forcing due to the [..[136]]nitric acid kinetic update, strictly as it relates to changes in atmospheric composition simulated by GEOS-Chem.

Input to PORT was compiled using output from the GEOS-Chem simulations. An instantaneous tracer time-series output was created for every 73rd time step, which resulted in [..[137]]output generated every 2,190 minutes. This output schedule enabled a balance of sampling all seasons, day and night occurrences, output files sizes, and overall computational strain. Conley et al. (2013) found such a sub-sampling routine to have less than a 0.1% relative error in the radiative flux when compared to a PORT simulation using every time sample. [..[138]]The radiative flux is defined as the net change in net downward solar and terrestrial (combined) radiation. Initial analysis of the GEOS-Chem output indicated that the main driver of instantaneous radiative forcing was tropospheric ozone, and to a lesser extent[..[139]], sulfate aerosols. The instantaneous radiative forcing simulation was carried on for a full year to allow for a calculation of a global annual average change in instantaneous radiative forcing. While the GEOS-Chem evaluation was limited to the time period of the INTEX-A campaign, the radiative effects portion of this evaluation had no such limitations.

[130] removed: short-lived climate forcers in the atmosphere. These changes result in variances in the radiative budget of the atmosphere and will change the predicted forcing at the surface and top of the model domain. For the updates to the nitric acid mechanism, these changes

[131] removed: the

[132] removed: , which is a large contributor to the radiation balance of our atmosphere. To a lesser extent, changes in radiative effects due to the updated nitric acid mechanism include concentration differences of certain aerosols, such as sulfuric acid. Ultimately, as previous mentioned, a decrease in the reaction rate of nitric acid formation will increase tropospheric photochemical ozone production, which is largely limited by

[133] removed: availability. This would have a positive increase in radiative effects in the atmosphere and the intensity of such radiative changes will largely be spatially and temporally heterogenous. In addition, the nitric acid mechanism update can change the oxidation potential of the atmosphere. This change can affect the formation of aerosols and has a potential to vary the concentration and distribution of aerosols, such as sulfuric acid. This process has the potential of creating negative radiative effects.

[134] removed: utilized

[135] removed: By using this model , the direct radative

[136] removed: mechanism updatecan be quantified.

[137] removed: an

[138] removed: Radiative effects due to ozone, sulfate, organic and black hydrophilic and hydrophobic carbon, sea salt and dust were quantified using PORT. While the main drivers of the radiative effects due to the mechanism update will be driven by

[139] removed: sulfate aerosols, all of these variables were included due to availability

3 RESULTS

[..[140]]**Evaluation** of Updated Nitric Acid Chemistry on Atmopsheric Composition

In this section, the base case and HNO3 case models are compared to the INTEX-A observations, with a focus on [..[141]]NO_y and the partitioning of NO_y species. Each component is evaluated in 1 km vertical bins from the surface (0 km) to 10 km. [..[142]]Due to the high bias of total oxidized nitrogen ($NO_y = NO_x + PAN + HNO_3$) [..[143]][..[144]][..[145]]

[..[146]]

[..[147]][..[148]]throughout most of the troposphere (as evident in Figure 2a), the remaining evaluation [..[149]]will feature a NO_y normalization.

Figure 2 shows the concentration of total oxidized nitrogen (NO_y) and the fractional amount of its components (NO_x, PAN, and HNO_3). [..[150]][..[151]]For each 1 km bin, Figure 2 shows the mean (black dots), median (white lines) and 90% range (5%-95%) of the observed (grey bars) and simulated values (base: blue, HNO3: red). The dots that represent the simulated means are black if the model mean is consistent with the observations (i.e., we cannot reject $H_{0,1}$ and $H_{0,2}$) and blank if the model mean is not statistically consistent with observations. Figure 2a shows that NO_y performance changes as a [..[152]]function of altitude. [..[153]]From 0-8 km[..[154]][..[155]][..[156]], both models feature statistically significant high biases of their mean values. As well, simulated NO_y is less concave than observed[..[157]], especially in the mid-troposphere, where observed values are at their minimum.

[..[163]][..[164]][..[165]]Between 8 and 10 km, the updated chemistry improves the partitioning predictions of NO_x, HNO_3, and PAN. For NO_x, [..[166]]both cases are low-biased from 8 to 10 km; however, the HNO3 case shows [..[167]]improvements. For HNO_3, both the base and HNO3 cases are high-biased from 8 to 10 km, but once again, the HNO3 case shows [..[168]]improvements. In fact, the 8 to 9 km [..[169]]observed and simulated mean values

[140] removed: Aircraft
[141] removed: ozone, nitrogen, and nitrogen partitioning
[142] removed: Initial evaluation
[143] removed: shows a high bias associated with
[144] removed: production from lightning. **??** displays the vertical emission profile of lightning in the model and a general overprediction of
[145] removed: can be seen in 2a.
[146] removed: Lightning emission profiles (VHF-2004 and SADS-2006).
[147] removed: Since a high bias exists for
[148] removed: throughout much of the atmosphere
[149] removed: of ozone, nitrogen and nitrogen partitioning from the updated mechanism
[150] removed: Each of the components are shown as a normalized percentage of
[151] removed: .
[152] removed: functional
[153] removed: Near the surface (0-3
[154] removed:) and from 5-8
[155] removed: , all the models are consistent with observations. Simulated
[156] removed: , however,
[157] removed: and all the models are high-biased from 2 to 7
[163] removed: The target of improved chemistry is above 8
[164] removed: , so the biases below 7
[165] removed: will be addressed separately.
[166] removed: the
[167] removed: significant
[168] removed: significant improvements. This is especially seen in
[169] removed: bin, where

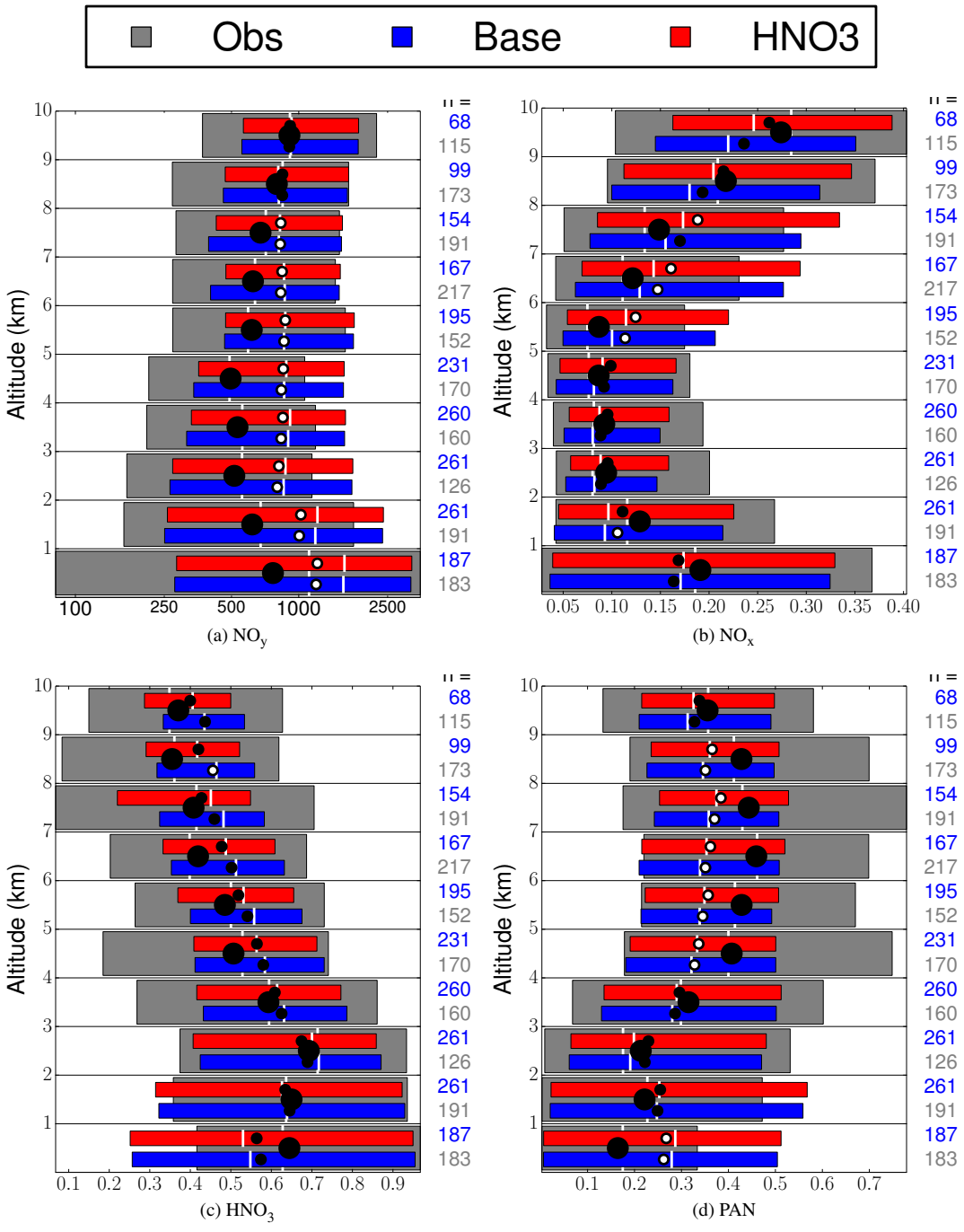

Fig. 2. Model evaluation at 10 1-km [..[158]]vertical bins. Each panel shows the 5^{th} to 95^{th} percentile range (box), median (white line), and mean (circle) for observations (grey), the base case (blue) [..[159]]and the HNO_3 case (red). When the mean circle for the predictions is filled in, the mean values between the observations and the predictions [..[160]]are not statistically different. The time period of these values matches the [..[161]]INTEX-A time period. [..[162]]The number of observations (black) and model points (blue) per 1 km bin are detailed in the margin.

no longer show [..[170]]statistically significant differences. For PAN, Figure [..[171]][..[172]][..[173]]2d shows more

[170]removed: statistical
[171]removed: 2c shows that the two cases are statistically consistent with observations from 0 to 10
[172]removed: , with an exception of the base case in this 8 to 9

incremental improvements in the upper troposphere. On an overall basis, the HNO3 case [..[174]][..[175]][..[176]][..[177]]

[..[178]][..[179]][..[180]][..[181]][..[182]]provides slight improvements in model performance of NO_y [..[183]][..[184]][..[185]][..[186]][..[187]][..[188]]

[..[189]][..[190]][..[191]][..[192]][..[193]][..[194]][..[195]][..[196]][..[197]][..[198]]partitioning in the upper troposphere.

When addressing [..[199]]nitrogen partitioning in the middle and lower troposphere, Figure 2b shows that both models underpredict NO_x [..[200]]partitioning from 0 to 2 km. [..[201]]However, when viewing Figure A8b, it is seen that predicted NO_x concentrations have high biases. Therefore, this partitioning bias is likely the result of high biased total NO_y concentrations. Nonetheless, the HNO3 case decreases the simulated low-bias [..[202]]for NO_x partitioning. The HNO3 case improves the predictions of HNO_3 partitioning throughout most of the middle and lower troposphere but, significant improvements [..[203]]in predicted NO_x [..[204]]and NO_y concentrations are needed to help alleviate the overall bias. For PAN[..[205]], Figure 2d shows that both scenarios predict high speciation at the surface [..[206]]and low speciation in the middle troposphere. However, throughout the middle troposphere, the HNO3 case increases the PAN normalized fraction, which improves model partitioning predictions.

Using the updated chemistry also exacerbates an existing high bias of ozone (not shown). The base

[173]removed: bin
[174]removed: improves model performance and is consistent with observations at all levels. For
[175]removed: , the HNO3 case improves predictions at all levels above 3
[176]removed: , though there are many bins of statistically significant low bias between 4 and 10
[177]removed: . However, this is seen in both simulated scenarios and is improved with the HNO3 case.
[178]removed: Unlike
[179]removed: ,
[180]removed: , and
[181]removed: , using the udpated chemistry exacerbates an existing high-bias. The base case ozone predictions are high-biased throughout most of the troposphere (excluding 1 to 3
[182]removed:). The high-bias for ozone is likely the result of over-predictions
[183]removed: and
[184]removed: . Figure 2a shows
[185]removed: over-prediction from 0 to 8
[186]removed: . The high-biased
[187]removed: is well correlated with a high-bias seen for
[188]removed: that extends throughout the same vertical structure.
[189]removed: The high-biased
[190]removed: may be the result of lightning emissions that are highly uncertain. GEOS-Chem emits
[191]removed: , produced from lightning flashes, according to a vertical profile published by Ott et al. (2010) shown in Fig. **??**. The lightning profie shows a distinct similarity between normalized
[192]removed: biases, as previously discussed. A high bias exists in the altitudes of 5 to 8
[193]removed: , which corresponds to an area of high lightning flashes. The ratio of freshly emitted
[194]removed: to
[195]removed: shows a distinct similarity with the bi-modal lighting profiles observed by Ott et al. (2010) and recommend by Allen et al. (2011). Using a bi-modal distribution that would redistribute
[196]removed: emissions from the middle troposphere to the upper and lower troposphere could improve the predictions. Overall, this update would improve the profile of
[197]removed: and its component species, but would likely have to be accompanied by a downward revision to remove the
[198]removed: high-bias
[199]removed: the
[200]removed: concentrations
[201]removed: Though, once again, when normalized to
[202]removed: . On a concentration basis, high bias exists for most species of
[203]removed: require the downward revision of
[204]removed: , which is driving the over predictions of
[205]removed: in the lower atmosphere
[206]removed: , as well

case ozone predictions are high-biased throughout most of the troposphere and are likely due to over-predictions of NO_y and NO_x. This may be the result of lightning emissions, which are highly uncertain and will be discussed later. Another important observation from Figure 2 is that NO_y partitioning is altitude dependent. [..[207]][..[208]][..[209]][..[210]][..[211]][..[212]][..[213]]In the middle troposphere, NO_x [..[214]]concentrations and partitioning are biased high (both [NO_x] and NO_x:NO_y). In the middle and upper troposphere, HNO_3 [..[215]]concentrations and partitioning are also biased high and likely a function of the similar high bias seen for NO_x. However, PAN is biased high near the surface (both [PAN] and PAN:NO_y[..[216]]), but generally consistent with observations on a concentration basis and low biased on a partitioning basis in the middle [..[217]]to upper troposphere.

[..[218]]of Updated Chemistry]Radiative Effects [..[219]][..[220]][..[221]]

[..[222]]of Updated Chemistry The SLCF that experienced changes between the base and HNO3 case were ozone and sulfate. As such, these climate forcers were the main focus of this radiative effects analysis. The global annual average [..[223]]instantaneous radiative forcing at the surface and top of the model due to the updated nitric acid [..[224]]mechanism was 6.7 mW/m^2 [..[225]]and 27.8 mW/m^2[..[226]], respectively. For PORT, the top of the model [..[227]]is 2.194 hPa. [..[228]][..[229]]The increase in ozone concentrations caused an increase in radiative flux at the surface and the top of the model [..[230]]of 10.4

[207] removed: Near the surface,
[208] removed: is biased high (
[209] removed: and
[210] removed: :
[211] removed:) and
[212] removed: is biased low as a fraction of
[213] removed: .
[214] removed: is
[215] removed: concentration is biased high , but the
[216] removed: is only biased high
[217] removed: and
[218] removed: The PORT simulations had a spin-up period of 4-months to allow for radiative equilibrium due to the atmospheric perturbation. Following the spin-up period, the simulation was carried on for a full year to allow a calculation of a
[219] removed: Evaluation
[220] removed: As previously mentioned, an offline radative transfer model (PORT) was run, utilizing the output generated from the GEOS-Chem GCM. The input to this offline model included ozone , sulfate, organic and black hydrophilic and hydrophobic carbon, sea salt and dust. While many of these variables were not expected to be changed as a result of this mechanism update, each were included due to their availability. Each of these climate forcing variables were analyzed individually to determine the radiative effects associated with each climate variable. The complete difference associated with the mechanism update was also analyzed. As hypothesized, the results showed that ozone was the strongest contributor to surface and top of atmosphere direct radiative effects , with smaller and localize effects also observed for simulated differences in sulfate aerosols. These variables changes are due to the
[221] removed: cycling that produces photochemical ozone and the changing atmospheric oxidation potential that the mechanism enables. The spatial and vertical changes, which further substantiate this assessment will be discussed further in the following section.
[222] removed: The PORT simulations had a spin-up period of 4-months to allow for radiative equilibrium due to the atmospheric perturbation. Following the spin-up period, the simulation was carried on for a full year to allow a calculation of a
[223] removed: change in radiative forcing . In total, this method enabled a global annual average radiative effects determination that included all seasons; and the simulation time step allowed an even analysis of day and night forcings. As previously mentioned, the time step for this analysis was every 2,190 minutes; which allowed a balance of computational strain and even season/daylight sampling routines. The global annual averaged change in radiative flux, including both solar and terrestrial radiation, at the surface from
[224] removed: reaction rate was 6.8
[225] removed: . The global annual averaged change in radiation flux at the effective top of the atmosphere was 27.9
[226] removed: . The effective top of the atmosphere, in reality, is
[227] removed: , which
[228] removed: As simulated, these values were driven strictly by the ozone and sulfate aerosol climate variables. Due to the increases in tropospheric ozone , the resulting change in radiative effects from ozone were a net positive gain. These increases were 31.1
[229] removed: at the
[230] removed: and

mW/m^2 [..[231]]and 31.0 mW/m^2, respectively. Similar to [..[232]]ozone, there was a net increase in sulfate [..[233]]aerosols, which occurred mainly in the lower troposphere [..[234]]and over landmasses. These increases resulted in a net decrease in [..[235]]instantaneous radiative forcing, driven by the reflectance of incoming solar radiation. The decreases were -3.4 mW/m^2 [..[236]]and -3.1 mW/m^2 at the surface and top of the model[..[237]][..[238]], respectively.

[..[239]][..[240]]Figure 3 and Figure 4 corroborate that ozone was the stronger contributor to surface and top of model [..[241]]

direct instantaneous radiative forcing, with more localized effects observed for sulfate. The range of the colorbars in the two respective Figures are similar, allowing for a comparison of the magnitude and spatial differences between the two SLCF. In total, Figure 3 displays the annual [..[242]]average instantaneous radiative forcing due to the changes in ozone from the updated mechanism [..[243]]at the surface, top of model, and the net atmospheric forcing. The net atmospheric forcing is defined as the top of the atmosphere radiative forcing minus the surface radiative forcing and has strong influences on regional precipitation (Shindell et al., 2012).

Figure 3 shows that there is a global increase in [..[244]]instantaneous radiative forcing due to the [..[245]]increases in ozone concentrations. In addition, [..[246]]the instantaneous radiative forcing simulations indicate the maximum increases occur in the [..[247]]mid-latitudes. Figure 3 also shows that higher values of instantaneous radiative forcing occur at the top of [..[248]]model, when compared to the surface. [..[249]]This leads to a net increase in the atmospheric forcing, which is [..[250]]shown in the third panel of Figure 3. The maximum of this value is above the equator and tapers off towards either pole.

[231] removed: at the surface
[232] removed: tropospheric
[233] removed: aersols
[234] removed: . This will be further discussed in the following section. However, in comparison to tropospheric ozone, this
[235] removed: radiative effects. These decreases were -3.0
[236] removed: at the
[237] removed: and -3.3
[238] removed: at the surface
[239] removed: To put these global annual average values into perspective, the Intergovernmental Panel on Climate Change (IPCC) Assessment Report 5 (AR5) estimated that the total radiative forcing since pre-industrial times for ozone to be
[240] removed: . The values from these results cannot be directly applied to these IPCC values since the IPCC values are estimated to occur at the troposphere, as is the definition of radiative forcing. However, it can be assumed that the values from this study would result in a net flux change at the troposphere to be somewhere between the simulated
[241] removed: values that were obtained. While the concentrations of tropospheric ozone have many determinants beyond the kinetic rate of nitric acid formation, the comparison of model predictions to published values of historical ozone forcing enables a comparative base line to analyze results against.
[242] removed: averaged spatial distribution of radiative effects
[243] removed: . As seen, there is largely a net
[244] removed: radiative forcing, which was hypothesized,
[245] removed: global increases of tropospheric ozone resulting from the mechanism update
[246] removed: it is observed that the
[247] removed: mid-latitude regions, with a slight decrease along the equator between the two mid-latitude regions. Also, a larger magnitude of forcing occurs
[248] removed: atmosphere
[249] removed: The net
[250] removed: the spatial plot at the bottom of the figure, is defined as the top of the atmosphere minus the surface forcing and has an influence on regional precipitation (Shindell et al. (2012)). As seen in this portion of Figure 3, the atmospheric forcing effects were entirely positive, with a maximum value situated near the equator . It is hypothesized that this result would cause precipitation increases in this portion of the world, which has the potential to further perturb the global radiation balance through indirect effects, which were not included in this simulation.

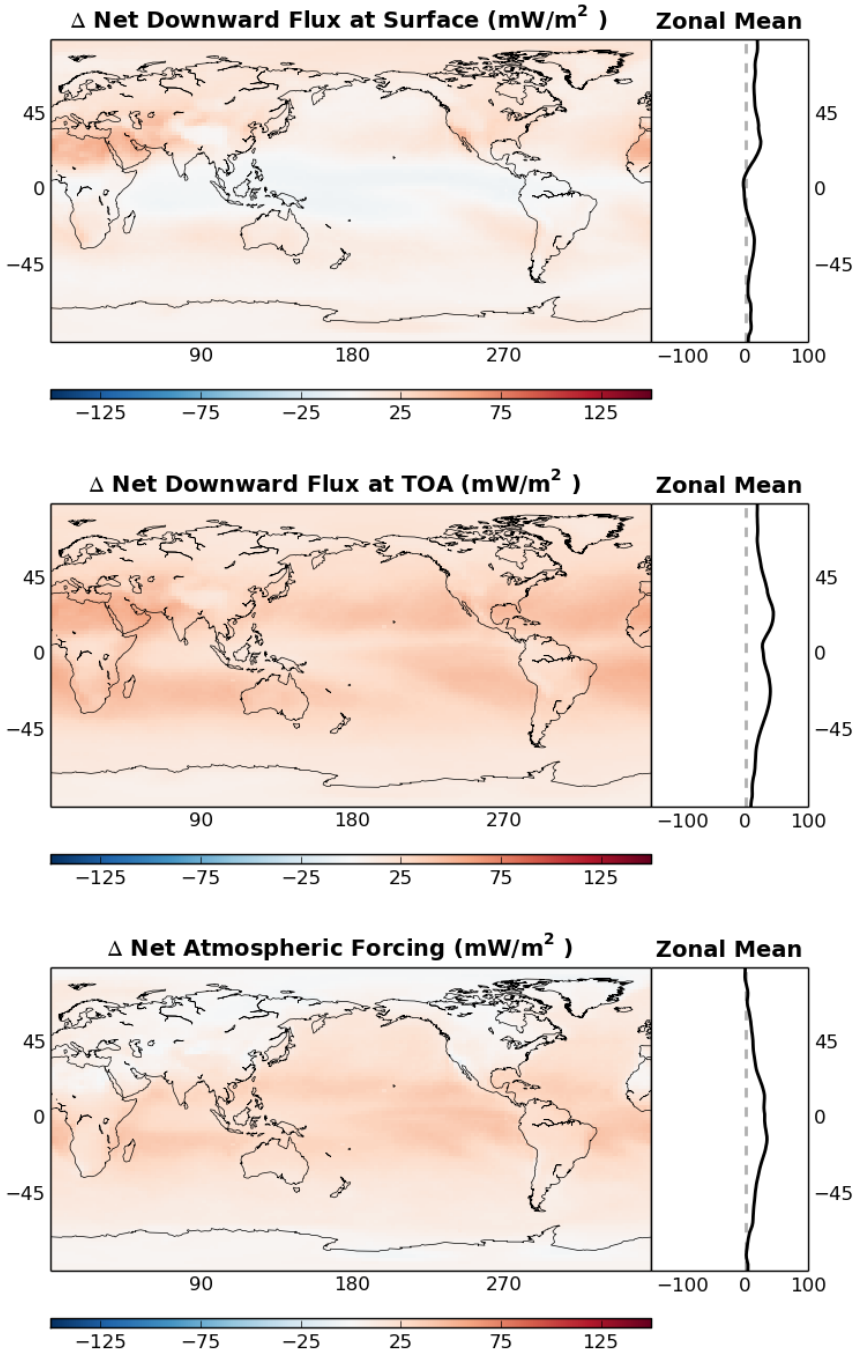

Fig. 3. [..[251]]Annual averaged instantaneous radiative forcing, in mW/m^2, at the surface (top) and top of the model (middle) for ozone. Net downward atmospheric forcing is shown in the bottom plot for ozone. Unlike the chemical mechanism evaluation, this simulation spanned a full year to enable an annual averaged calculation.

Figure 4 [..[252]]displays the annual average instantaneous radiative forcing due to the changes in [..[253]

[252]removed: shows the radiative effects resulting from

[253]removed: the atmospheric sulfate concentrations. These changes are a function of the localized adjustments in oxidative capacity due to the decrease in oxidation of

]sulfate from the updated mechanism at the surface, top of model, and the net atmospheric forcing. In contrast to Figure 3 and the [..[254]]global increase in radiative flux associated with ozone, the simulated [..[255]]instantaneous radiative forcing associated with sulfate [..[256]]was localized. These areas were predominantly over land, with the heaviest changes above highly polluted areas, such as China and the Northeast United States. Also in contrast to the [..[257]]instantaneous radiative forcing associated with ozone, the radiative effects associated with [..[258]]sulfate strictly resulted in decreases to the radiative flux. [..[259]][..[260]]

Spatial [..[262]]Variations of Short-Lived Climate Forcers

This section describes the spatial concentration changes [..[263]]of the SLCF studied in this analysis, as well as some of the species that play a role in their variations (HNO_3, NO_x[..[264]][..[265]][..[266]]). In total, changes in their horizontal and vertical patterns[..[267]][..[268]][..[269]], due to the revised mechanism, will be shown. Fig. 5 and Fig. 6 show that the increases in ozone occurred globally, with maximum increases occurring in the [..[270]]upper mid-latitudes, spanning the entire vertical domain. Vertically, most of the ozone changes occurred in the free troposphere, above the planetary boundary layer. For sulfate, Fig. 5 indicates that the surficial changes were nearly all [..[271]]over landmasses that are traditionally locations of high pollution. However, [..[272]]when viewed in the vertical domain, Fig. 6 shows that the changes to sulfate concentrations were limited to areas near the surface and in the upper mid-latitudes.

Figure 5 shows that the localized concentration changes to HNO_3 and NO_x in the surfacial layer had an inverse relationship with one another, and occurred in the same localized regions as the concentration changes to sulfate. When reviewing Reaction 1, this inverse relationship is expected. However, the decrease in the formation of nitric acid due to this mechanism update would [..[273]]lead to an expected increase in NO_x, which is not shown in Figure 5. When viewing Figure 6, it is seen that this phenomenon is limited to the surface and quickly [..[274]]changes throughout the rest of the troposphere. This is likely due to an increase in heterogeneous nitrogen chemistry on the surface of the locally increased sulfate

[254]removed: near global radiative effects
[255]removed: radiative changes
[256]removed: aerosols were only localized; and the local areas were only above landmasses
[257]removed: radiative effects assoicated
[258]removed: the sulfate aerosols resulted in net decreases in
[259]removed: The longitudinally averaged portion of the plot shows near zero values at all latitudes due to the strongly localized nature of these changes. It is hypothesized that these localized, traditionally polluted areas, are limited in their capacity to oxidize
[260]removed: and the increase in hydroxyl radicals resulting from this mechanism update allowed the increase in production of sulfate aerosols.
[262]removed: Assessment
[263]removed: due to the revised chemistry kinetics. The analysisincludes simulated changes to
[264]removed: ,
[265]removed: and
[266]removed: , on both
[267]removed: . As seen in Figure **??**, which displays the difference in
[268]removed: and
[269]removed: concentrations at the surface between the HNO3 and Base Case simulations,
[270]removed: localized variations in both species had an obvious inverse relationship, and
[271]removed: localized over landmasses
[272]removed: the localized directional changes are counter intuitive to the assumed directional change that the
[273]removed: create. These directional changes are strictly
[274]removed: change throughout the troposphere, as shown in Figure **??**. Figure **??**

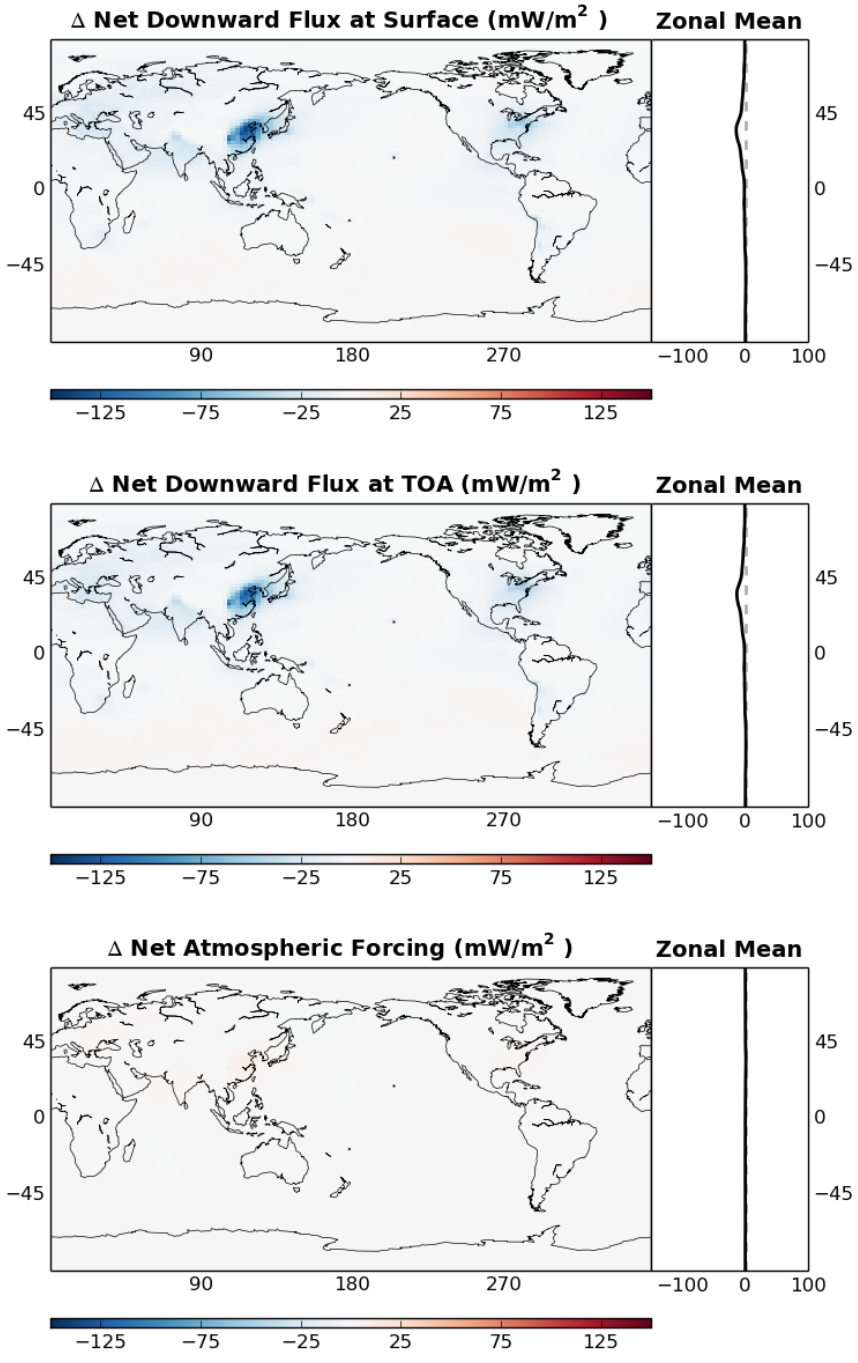

Fig. 4. [..[261]]Annual averaged instantaneous radiative forcing, in mW/m^2, at the surface (top) and top of model (middle) for sulfate aerosols. Net downward atmospheric forcing is shown in the bottom plot for sulfate aerosols. Unlike the chemical mechanism evaluation, this simulation spanned a full year to enable an annual averaged calculation.

aerosols (Bell et al., 2005; Liao et al., 2004). Figure 6 shows that, once again, the [..[275]]concentrations

[275] removed: directional

changes for HNO_3 and NO_x are inversely [..[276]]related throughout the troposphere[..[277]][..[278]]. It should also be noted that [..[279]]the strongest differences in HNO_3 and NO_x concentrations occurred in the upper troposphere, [..[280]]where the updated chemistry plays a stronger role.

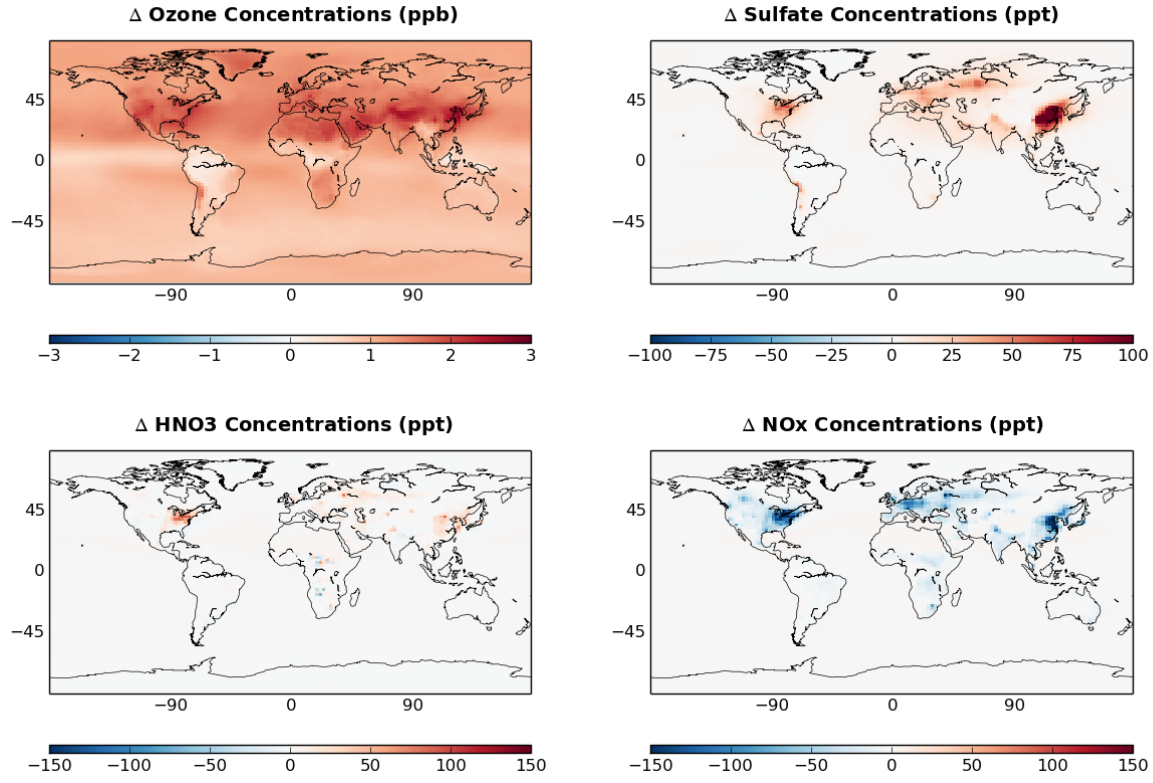

Fig. 5. Difference in mean ozone, sulfate, nitric acid and NO_x mixing ratios mixing ratios between the HNO3 and Base Case simulations for the surface layer. The simulation period spanned an entire year.

[..[282]]

4 DISCUSSION ON CONTINUED MODEL BIAS

While the updated chemistry helped improve the predictions of speciated NO_y at most levels of the atmosphere, [..[283]]several model biases are still observed. One such bias is the over predictions of NO_x

[276]removed: proportional
[277]removed: , and the only areas of
[278]removed: increase occur in the upper mid-latitudes at the surface
[279]removed: stronger
[280]removed: which was the targeted zone of evaluation for this project
[282]removed: As shown in Figure **??**, the changes in the spatial distribution of ozone at the surface resulted in near global increases. A majority of the ozone changes occurred in the upper mid-latitudes and spanned the entire vertical atmosphere, as shown in Figure **??**. Vertically, most of the ozone changes occurred in the free troposphere
[283]removed: above the planetary boundary layer. The previous hypothesis that the changes in sulfate radiative effects were a result of changing oxidation potential were further review by looking at the spatial distribution of sulfate aerosol changes, as well. When reviewing Figure **??**, it is seen that the horizontal changes in sulfate at the surface occurred in the same localized regions as the surficial changes to

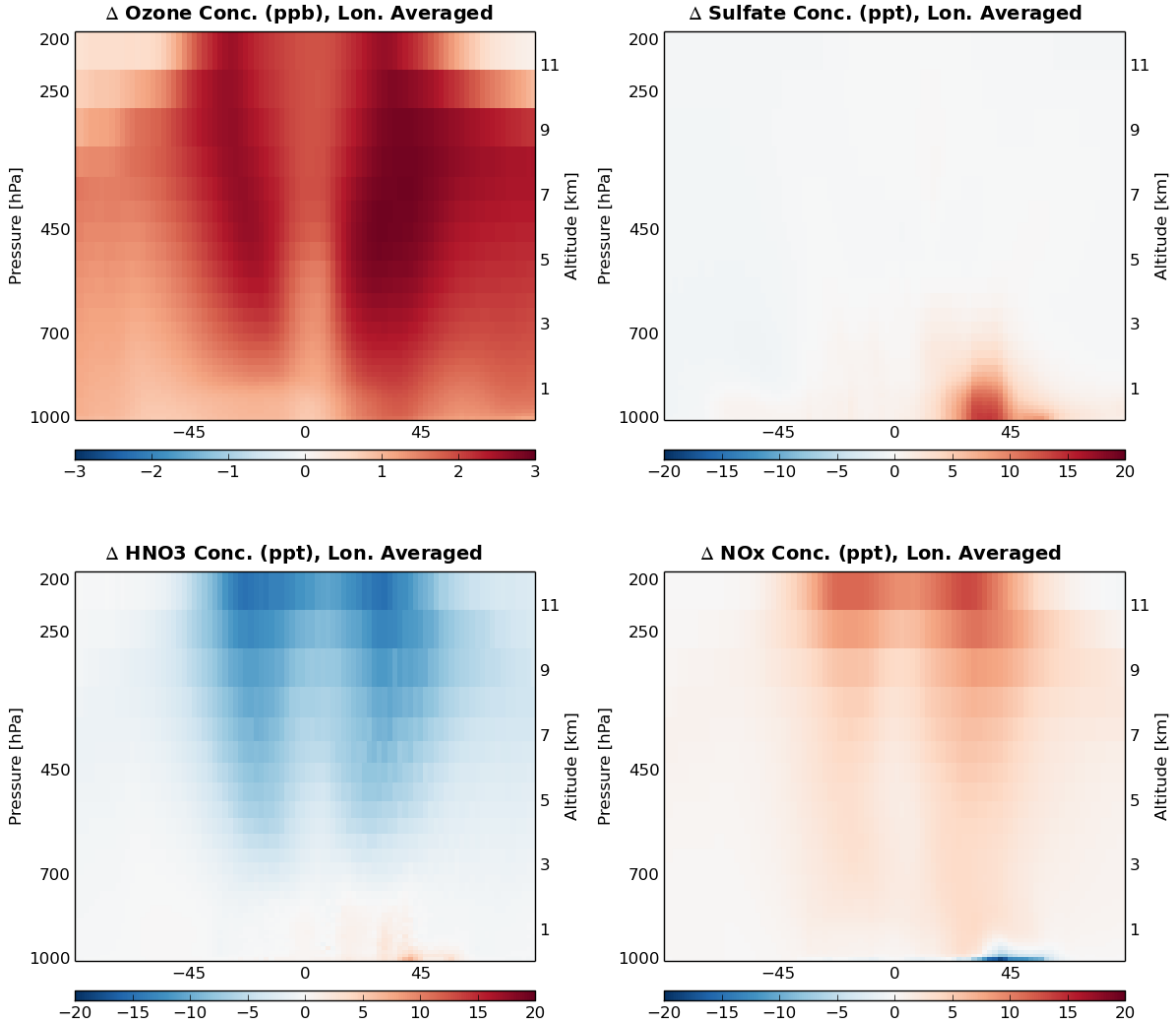

Fig. 6. Vertical difference in mean [..[281]]nitric acid, NO_x, ozone and sulfate mixing ratios between the HNO3 and Base Case simulations (longitudinally averaged values). The simulation period spanned an entire year.

and [..[284]][..[285]]NO_y in the middle troposphere. Sources of NO_x [..[286]]
[..[287]][..[288]]
[..[289]][..[290]]
[..[291]][..[292]]in these areas include convectively lofted anthropogenic NO_x, lightning, transport from
320 the stratosphere and aircraft emissions (Jaegl et al., 1998b; Hudman et al., 2007). In this study, the

[284]removed: . When viewed on a vertical basis, Figure **??** shows the the vertical changes to sulfate aerosol concentrations strictly occurred near the surface and did not follow the same trends as
[285]removed: and
[286]removed: , which had large differences throughout the troposphere.
[287]removed: Difference in mean
[288]removed: and Sulfate mixing ratios between the HNO3 and Base Case simulations for the surface layer.
[289]removed: Vertical difference in mean
[290]removed: and Sulfate mixing ratios between the HNO3 and Base Case simulations (longitudinally averaged values).
[291]removed: Literature updates to the
[292]removed: reaction rate requires reanalysis

observations are filtered to exclude stratospheric intrusion and Allen et al. (2011) found that the impact of aircraft NO emissions on upper tropospheric NO_x during a flight path from the INTEX-A campaign were generally small. Though, it was stated that the impacts related to aircraft NO emissions are more evident in periods of low lightning NO_x (LNOx) emissions. This leaves either LNOx or convectively lofted anthropogenic NO_x as the main drivers of this bias. Hudman et al. (2007) studied upper tropospheric NO_x during the INTEX-A campaign using GEOS-Chem and found that lightning was the dominant factor in upper tropospheric NO_x bias. Though, the largest bias from their study was in regions of the upper troposphere above the domain used in this study and they were low biased. As well, their version of GEOS-Chem [..[293]]utilized an older vertical release profile of LNOx. Newer GEOS-Chem versions, such as the one used in this study, [..[294]][..[295]][..[296]][..[297]]utilize the vertical release profiles developed by Ott et al. (2010). In these updated profiles, large portions of upper and lower tropospheric LNOx fractions were moved to the middle troposphere. Figure 7 displays the general vertical LNOx emission profile for the subtropical regions used in GEOS-Chem (Ott) and two other vertical LNOx emission profiles, which were used in Allen et al. (2011). While all LNOx vertical profiles display low fractional emissions near the surface, which was one of the significant updates made in Ott et al. (2010), variations do exist in the middle troposphere. These areas happen to be locations where high bias of NOx/NOy partitioning and NOx concentrations mainly occur. It is hypothesized that a bi-modal lighting profile, similar to some of the observations by Ott et al. (2010) and used by Allen et al. (2011), which include a redistribution of some of the NO_x [..[298]][..[299]][..[300]][..[301]][..[302]]

[..[303]][..[304]][..[305]][..[306]][..[307]]emissions from the middle troposphere to the upper troposphere, [..[308]]could improve the predictions. In addition to the improvements in NO_x predictions, this update could also improve NO_y [..[309]]concentrations and HNO_3[..[310]][..[311]][..[312]]/PAN partitioning.

[293] removed: model performance and its sensitivity to the resulting chemistry. In

[294] removed: we have implemented updates to the GEOS-Chem chemistry and evaluated those updates during the INTEX-A observational campaign. Following an adjustment to this chemical mechanism, an evaluation of

[295] removed: , its components and the resulting effects on atmospheric direct radiative effects were analyzed. We find that the base model has a high bias for

[296] removed: , so

[297] removed: components (

[298] removed: ,

[299] removed: , and

[300] removed:) were evaluated as fractional components to determine how the mechanism effects speciation. Overall, the updated chemistry improves total oxidized nitrogen partitioning and decreases the termination of

[301] removed: through the formation of nitric acid. In addition, since the oxidation of

[302] removed: was decreases, a near global increase in ozone concentrations were seen. This increase resulted in changes to the oxidation potential of localized regions, which changes the concentration of resulting aerosol formation. All of these results have a relationship with the simulated radiation budget of the atmosphere.

[303] removed: The updated

[304] removed: chemistry improves simulated partitioning of

[305] removed: ,

[306] removed: , and

[307] removed: throughout most of the atmosphere. In

[308] removed: where this analysis was mainly targeting improved simulation results, the updated chemical mechanism improves modeled results for all

[309] removed: components above 8 km. In the middle troposphere,

[310] removed: and

[311] removed: also experience improvements in predictions; however, the updated chemistry exacerbates a base model bias for

[312] removed: that may be caused by the lightning emission profile.

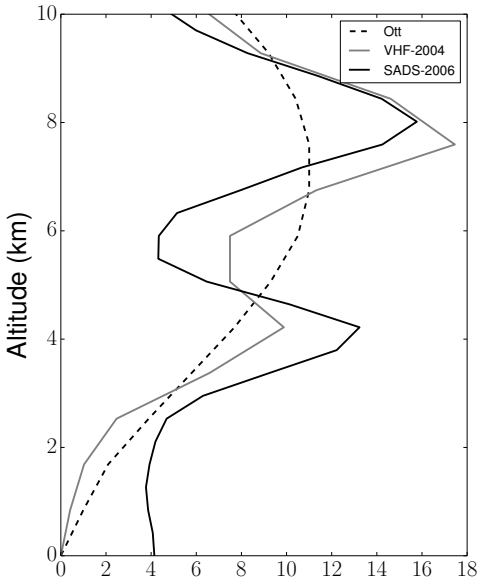

Fig. 7. Vertical lightning emission profiles. The Ott LNOx vertical emission profile is used by GEOS-Chem in the subtropical regions (Ott et al., 2010). The VHF-2004 and SADS-2006 LNOx vertical emission profiles are alternative LNOx emission profiles and were used in the study by Allen et al. (2011). The horizontal axis represents the fractional percentage of LNOx emitted.

[..[313]][..[314]][..[315]]

The simulated concentrations of PAN, which match observations relatively well in the middle [..[316]][..[317]][..[318]][..[319]]and upper troposphere, as seen in Fig. A8d, is most likely tied to the low-bias for acetaldehyde and [..[320]][..[321]][..[322]][..[323]]high-bias for HO$^{\cdot}$. The high-biased HO$^{\cdot}$ would preferentially remove fast reacting compounds, like acetaldehyde ($k_{\mathrm{HO}\cdot} = 4.63 \times 10^{-12} \times \exp(350/T)$), compared to acetaldehyde's precursors, ethane ($k_{\mathrm{HO}\cdot} = 7.6 \times 10^{-12} \times \exp(-1020/T)$) and ethanol ($k_{\mathrm{HO}\cdot} = 3.15 \times 10^{-14}$). This suggests, as did Millet et al. (2010), that there is not, in fact, a missing source of acetaldehyde. Instead, an imbalance caused by over-predicted sinks causes acetaldehyde underpredictions[..[324]], which lead to low $CH_3C(O)OO^{\cdot}$ radicals and reduced PAN formation. The updated chemistry used here exacerbates the HO$^{\cdot}$ bias [..[325]]and, in turn, typically lowers the model bias for PAN, which would not be as well simulated in circumstances with proper concentrations of HO$^{\cdot}$. More research is necessary to constrain this problem.

[313] removed: While the updated chemistry helped improve the predictions of speciated
[314] removed: at most levels of the atmosphere, several model biases are still observed. This includes over predictions of
[315] removed: and
[316] removed: troposphere and underpredictions for
[317] removed: at most altitudes. As mentioned previously, it is hypothesized that
[318] removed: , and in turn
[319] removed: , would be improved with an update to the lightning emission profile. The performance of
[320] removed: :
[321] removed: . The low-bias in
[322] removed: :
[323] removed: is caused by a
[324] removed: that
[325] removed: , andmore

[..[326]]Similar to the changes in oxidized nitrogen concentrations, the change in simulated ozone [..[327]]concentrations is modest. The updated model [..[328]]increases the availability of NO_x[..[329]][..[330]], which is generally the limiting species in tropospheric ozone production. Simulations using the updated chemical mechanism saw global increases of ozone throughout the troposphere, which increases the model bias. This further suggests that constraints on NO_x emissions are needed to improve modeled ozone concentrations.

5 CONCLUSIONS

Updates to the $NO_2 + HO^{\cdot}$ reaction rate, as suggested by Mollner et al. (2010) and Henderson et al. (2012), were implemented in GEOS-Chem and the resulting model performance was evaluated using observations from the INTEX-NA, Phase-A campaign. This evaluation considered total NO_y concentrations, NO_y partitioning, and the resulting direct instantaneous radiative forcing effects from this mechanism update. An initial comparison found that the base model had a high bias for NO_y. As such, NO_y components (NO_x, HNO_3, and PAN) were evaluated as fractional components to determine how the mechanism effects speciation. Overall, the updated chemistry improves oxidized nitrogen partitioning and decreased the termination of NO_x in the atmosphere through the formation of nitric acid.

In the upper troposphere, the [..[331]][..[332]]updated chemistry improves modeled results for the partitioning of all NO_y components. In the middle troposphere, HNO_3 and PAN also show improvements in predictions; however, the updated chemistry [..[333]]exacerbates a base model bias for NO_x. Results in the lower troposphere show increased model bias for HNO_3 and PAN. Therefore, additional work is recommended to understand the partitioning of NO_x in the middle [..[334]]troposphere and HNO_3 and PAN near the surface.

A near global increase in ozone concentrations and localized changes in sulfate concentrations also resulted from this update. These variations in short-lived climate forcers have an immediate impact on the amount of trapped energy in the atmosphere. Ozone concentration increases were a result of increased NO_x availability whereas sulfate increases, which were spatially heterogeneous, are hypothesized to be a result of changes in atmospheric oxidation capacity. Variations in the atmospheric oxidation capacity result from a decrease in the formation of HNO_3, which requires NO_2 and $HO^{\cdot}$. This increase in $HO^{\cdot}$ enables an increase in the oxidation of SO_2 to SO_4. Sulfate generally increased over traditionally polluted areas, such as Eastern China and the Northeastern United States. Corresponding decreases in HNO_3 were simulated throughout the troposphere above these locations, which corrobo-

[326] removed: Like the improvements
[327] removed: sensitivity
[328] removed: uses
[329] removed: more efficiently and, therefore, is more responsive to incremental reductions of
[330] removed: . In response to reduced
[331] removed: sensitivity of predicted
[332] removed: concentrations was never more than a couple percent different based on updated chemistry . At the surface, where air quality is the primary concern,
[333] removed: increases sensitivity the least and the largest changes are seen at the mid-latitudes
[334] removed: to upper troposphere

rates the hypothesis that the sulfate increases were likely a result to the changing atmospheric oxidation capacity. [..[335]]

The [..[336]]radiative effects due to the changes in ozone and sulfate [..[337]]concentrations were evaluated using an offline radiative transfer model[..[338]]. The annual average instantaneous radiative forcing was largely driven by the changes in ozone concentrations, with slight effects from sulfate aerosols. Overall, [..[339]]an annual average instantaneous radiative forcing of 6.7 mW/m2 and [..[340]]27.8 mW/m2 was [..[341]]simulated for the surface and the top of [..[342]]model, respectively. [..[343]]The radiative effects from ozone were seen globally, with maximum variances [..[344]]in the mid-latitudes. In contrast, the radiative effects resulting from the changes in sulfate [..[345]]were generally limited to areas over landmasses[..[346]][..[347]][..[348]].

[..[349]]To put these global annual average values into perspective, the Intergovernmental Panel on Climate Change (IPCC) Assessment Report 5 (AR5) estimated that the total radiative forcing since pre-industrial times due to ozone is 350 mW/m^2. While the concentrations of tropospheric ozone have many determinants beyond the kinetic rate of nitric acid formation, the comparison of model predictions to published values of historical ozone forcing enables a comparative base line to analyze these results against. As well, additional radiative effects can be expected due to this mechanism update. In the tropics, where a net positive increase in atmospheric forcing is simulated, additional atmospheric responses and feedbacks are likely to occur. These feedbacks include changes in atmospheric moisture and cloud cover. Since the radiative transfer model used in this evaluation was offline, these calculations were not included and should be considered in future work.

Overall, this study demonstrates that updates to the [..[350]]nitric acid chemical mechanism generally improves oxidized nitrogen partitioning performance in GEOS-Chem throughout the troposphere. It should be noted, however, that this model evaluation is based on a model that is already high-biased for NO_y concentrations [..[351]]throughout a majority of the troposphere. As such, improvements to the global emission

[335]removed: The larger differences in the upper troposphere are most likely due to long-range transport. As a result to these changes in tropospheric ozone, simulated climate forcing due to this climate variable were evaluated.

[336]removed: changing atmospheric chemistry, mainly relating to

[337]removed: aerosols, experienced changes due to this mechanism update. By utilizing

[338]removed: , the radiative effects resulting from this kinetic update were quantified. Raditiave effects were seen in both the solar and terrestrial forms of the radiation spectrum, and were mainly caused by differences in ozone

[339]removed: a positive net flux of 6.8

[340]removed: a positive net flux of 27.9

[341]removed: quantified

[342]removed: the atmosphere

[343]removed: Ozone contributed radiative effects in both the solar and terrestrial forms of radiative energy while sulfate only contributed effects in the solar form through scattering processes.

[344]removed: seen

[345]removed: concentrations were

[346]removed: , and has the strongest influences over China and the Northeast United States. Overall, a positive net flux of 10.4

[347]removed: and a negative net flux of 3.3

[348]removed: was quantified for the surface for ozone and sulfate aerosols, respectively

[349]removed: This

[350]removed: chemical mechanism improves precursor performance without drastically changing the policy implications of the model. The sensitivity of the model, as evaluated in this paper, however, is relative to

[351]removed: . Improvements

inventories could [..[352]][..[353]][..[354]]significantly help the overall modeled concentrations of total oxidized nitrogen.

Acknowledgements. Special thanks Rob Pinder [..[355]]and Farhan Akhtar, as well as Melody Avery, Bruce Anderson, John Barrick, Donald Blake, [..[356]]Ed Browell, Anthony Clarke, Ron C Cohen, Glenn Diskin, Alan Fried, Brian Heikes, Greg Huey, Jim Podolske, Glen Sachse, Rick Shetter, Hanwant Singh, [..[357]]Robert Talbot, David Tan, Stephanie Vay, Rodney Weber, Paul Wennberg, William Brune, Daniel Jacob, James Crawford and the rest of the INTEX-A team for the [..[358]]DC-8 observational data.

In addition, the authors would like to thank two anonymous reviewers whose valuable comments helped to substantially improve this manuscript.

REFERENCES

Allen, D. J., Pickering, K. E., Pinder, R. W., Henderson, B. H., Appel, K. W., and Prados, A.: Impact of lightning-NO on Eastern United States photochemistry during the summer of 2006 as determined using the CMAQ model, Atmospheric Chemistry and Physics Discussions, 11, 17 699–17 757, doi:10.5194/acpd-11-17699-2011, 2011.

Atkinson, R., Baulch, D. L., Cox, R. A., Crowley, J. N., Hampson, R. F., Hynes, R. G., Jenkin, M. E., Rossi, M. J., and Troe, J.: Evaluated kinetic and photochemical data for atmospheric chemistry: Volume I - gas phase reactions of Ox, HOx, NOx and SOx species, Atmospheric Chemistry and Physics, 4, 1461–1738, doi:10.5194/acp-4-1461-2004, 2004.

Bell, N., Koch, D., and Shindell, D. T.: Impacts of chemistry-aerosol coupling on tropospheric ozone and sulfate simulations in a general circulation model, Journal of Geophysical Research, 110, doi:10.1029/2004JD005538, 2005.

Bertram, T. H., Perring, A. E., Wooldridge, P. J., Crounse, J. D., Kwan, A. J., Wennberg, P. O., Scheuer, E., Dibb, J., Avery, M., Sachse, G., Vay, S. A., Crawford, J. H., McNaughton, C. S., Clarke, A., Pickering, K. E., Fuelberg, H., Huey, G., Blake, D. R., Singh, H. B., Hall, S. R., Shetter, R. E., Fried, A., Heikes, B. G., and Cohen, R. C.: Direct Measurements of the Convective Recycling of the Upper Troposphere, Science, 315, 816–820, doi:10.1126/science.1134548, 2007.

Browne, E. C., Perring, A. E., Wooldridge, P. J., Apel, E., Hall, S. R., Huey, L. G., Mao, J., Spencer, K. M., Clair, J. M. S., Weinheimer, A. J., Wisthaler, A., and Cohen, R. C.: Global and regional effects of the photochemistry of CH3O2NO2: evidence from ARCTAS, Atmospheric Chemistry and Physics, 11, 4209–4219, doi:10.5194/acp-11-4209-2011, 2011.

Chameides, W. L., Fehsenfeld, F., Rodgers, M. O., Cardelino, C., Martinez, J., Parrish, D., Lonneman, W., Lawson, D. R., Rasmussen, R. A., Zimmerman, P., Greenberg, J., Mlddleton, P., and Wang, T.: Ozone precursor relationships in the ambient atmosphere, Journal of Geophysical Research, 97, 6037, doi:10.1029/91JD03014, 1992.

Chen, D., Wang, Y., McElroy, M. B., He, K., Yantosca, R. M., and Le Sager, P.: Regional CO pollution and export in China simulated by the high-resolution nested-grid GEOS-Chem model, Atmospheric Chemistry and Physics, 9, 3825–3839, doi:10.5194/acp-9-3825-2009, 2009.

Cohan, D. S., Koo, B., and Yarwood, G.: Influence of uncertain reaction rates on ozone sensitivity to emissions, Atmospheric Environment, 44, 3101–3109, doi:10.1016/j.atmosenv.2010.05.034, 2010.

[352]removed: alter the relative sensitivities in this study, but conclusions were robust when used with two versions of the NEI (NEI99 not shown). The chemistry updates for the rate of

[353]removed: used in this study also need confirmation by more laboratory and field studies. The rate of

[354]removed: is key to the inorganic and organic chemical cycling that drives ozone production, and acceptance of updates to this rate will require a preponderance of evidence.

[355]removed: , Farhan Akhtarand to

[356]removed: William Brune,

[357]removed: and the INTEX

[358]removed: DC8

Conley, A. J., Lamarque, J.-F., Vitt, F., Collins, W. D., and Kiehl, J.: PORT, a CESM tool for the diagnosis of radiative forcing, Geoscientific Model Development, 6, 469–476, doi:10.5194/gmd-6-469-2013, 2013.

Dallmann, T. R. and Harley, R. A.: Evaluation of mobile source emission trends in the United States, Journal of Geophysical Research, 115, doi:10.1029/2010JD013862, 2010.

Donahue, N. M.: Atmospheric chemistry: The reaction that wouldn't quit, Nature Chemistry, 3, 98–99, doi:10.1038/nchem.941, 2011.

Fusco, A. C. and Logan, J.: Analysis of 19701995 trends in tropospheric ozone at Northern Hemisphere midlatitudes with the GEOS-CHEM model, Journal of Geophysical Research, 108, doi:10.1029/2002JD002742, 2003.

Guenther, A., Karl, T., Harley, P., Wiedinmyer, C., Palmer, P. I., and Geron, C.: Estimates of global terrestrial isoprene emissions using MEGAN (Model of Emissions of Gases and Aerosols from Nature), Atmospheric Chemistry and Physics, 6, 3181–3210, doi:10.5194/acp-6-3181-2006, 2006.

Henderson, B. H., Pinder, R. W., Crooks, J., Cohen, R. C., Carlton, A. G., Pye, H. O. T., and Vizuete, W.: Combining Bayesian methods and aircraft observations to constrain the HO + NO2 reaction rate, Atmospheric Chemistry and Physics, 12, 653–667, doi:10.5194/acp-12-653-2012, 2012.

Hudman, R. C., Jacob, D. J., Turquety, S., Leibensperger, E. M., Murray, L. T., Wu, S., Gilliland, A. B., Avery, M., Bertram, T. H., Brune, W., Cohen, R. C., Dibb, J. E., Flocke, F. M., Fried, A., Holloway, J., Neuman, J. A., Orville, R., Perring, A., Ren, X., Sachse, G. W., Singh, H. B., Swanson, A., and Wooldridge, P. J.: Surface and lightning sources of nitrogen oxides over the United States: Magnitudes, chemical evolution, and outflow, Journal of Geophysical Research, 112, doi:10.1029/2006JD007912, 2007.

Jacob, D. J., Logan, J. A., Gardner, G. M., Yevich, R. M., Spivakovsky, C. M., Wofsy, S. C., Sillman, S., and Prather, M. J.: Factors regulating ozone over the United States and its export to the global atmosphere, Journal of Geophysical Research, 98, 14 817, doi:10.1029/98JD01224, 1993.

Jacobson, M. Z.: Fundamentals of atmospheric modeling, Cambridge University Press, Cambridge, UK ; New York, 2nd ed edn., 2005.

Jaegl, L., Jacob, D. J., Brune, W. H., Tan, D., Faloona, I. C., Weinheimer, A. J., Ridley, B. A., Campos, T. L., and Sachse, G. W.: Sources of HOx and production of ozone in the upper troposphere over the United States, Geophysical Research Letters, 25, 1709–1712, doi:10.1029/98GL00041, 1998a.

Jaegl, L., Jacob, D. J., Wang, Y., Weinheimer, A. J., Ridley, B. A., Campos, T. L., Sachse, G. W., and Hagen, D. E.: Sources and chemistry of NO $_x$ in the upper troposphere over the United States, Geophysical Research Letters, 25, 1705–1708, doi:10.1029/97GL03591, 1998b.

Jaegl, L., Jaffe, D., Price, H., Weiss-Penzias, P., Palmer, P., Evans, M., Jacob, D., and Bey, I.: Sources and budgets for CO and O3 in the northeastern Pacific during the spring of 2001: Results from the PHOBEA-II Experiment, Journal of Geophysical Research, 108, doi:10.1029/2002JD003121, 2003.

Kopacz, M., Jacob, D. J., Fisher, J. A., Logan, J. A., Zhang, L., Megretskaia, I. A., Yantosca, R. M., Singh, K., Henze, D. K., Burrows, J. P., Buchwitz, M., Khlystova, I., McMillan, W. W., Gille, J. C., Edwards, D. P., Eldering, A., Thouret, V., and Nedelec, P.: Global estimates of CO sources with high resolution by adjoint inversion of multiple satellite datasets (MOPITT, AIRS, SCIAMACHY, TES), Atmospheric Chemistry and Physics, 10, 855–876, doi:10.5194/acp-10-855-2010, 2010.

Kuhns, H., Green, M., and Etyemezian, V.: Big Bend Regional Aerosol and Visibility Observational (BRAVO) Study Emissions Inventory, Desert Research Institute, 2003.

Liao, H., Seinfeld, J. H., Adams, P. J., and Mickley, L. J.: Global radiative forcing of coupled tropospheric ozone and aerosols in a unified general circulation model, Journal of Geophysical Research, 109, doi:10.1029/2003JD004456, 2004.

McKeen, S. A., Hsie, E.-Y., and Liu, S. C.: A study of the dependence of rural ozone on ozone precursors in the eastern United States, Journal of Geophysical Research, 96, 15 377, doi:10.1029/91JD01282, 1991.

Millet, D. B., Guenther, A., Siegel, D. A., Nelson, N. B., Singh, H. B., de Gouw, J. A., Warneke, C., Williams, J., Eerdekens, G., Sinha, V., Karl, T., Flocke, F., Apel, E., Riemer, D. D., Palmer, P. I., and Barkley, M.: Global atmospheric budget of acetaldehyde: 3-D model analysis and constraints from in-situ and satellite observations, Atmospheric Chemistry and Physics, 10, 3405–3425, doi:10.5194/acp-10-3405-2010, 2010.

Mollner, A. K., Valluvadasan, S., Feng, L., Sprague, M. K., Okumura, M., Milligan, D. B., Bloss, W. J., Sander, S. P., Martien, P. T., Harley, R. A., McCoy, A. B., and Carter, W. P. L.: Rate of Gas Phase Association of Hydroxyl Radical and Nitrogen Dioxide, Science, 330, 646–649, doi:10.1126/science.1193030, 2010.

Olivier, J., Berdowski, J., Peters, J., Bakker, J., Visschedijk, A., and Bloos, J.: Applications of EDGAR emission database for global atmospheric research, RIVM report 773301001 / NRP report 410 200 051, 2002.

Ott, L. E., Pickering, K. E., Stenchikov, G. L., Allen, D. J., DeCaria, A. J., Ridley, B., Lin, R.-F., Lang, S., and Tao, W.-K.: Production of lightning NOx and its vertical distribution calculated from three-dimensional cloud-scale chemical transport model simulations, Journal of Geophysical Research, 115, doi:10.1029/2009JD011880, 2010.

Parrish, D. D.: Critical evaluation of US on-road vehicle emission inventories, Atmospheric Environment, 40, 2288–2300, doi:10.1016/j.atmosenv.2005.11.033, 2006.

Sander, S., Abbatt, J., Barker, J., Burkholder, J., Friedl, R., Golden, D., Huie, R., Kolb, C., Kurylo, M., Moortgat, G., Orkin, V., and Wine, P.: Chemical Kinetics and Photochemical Data for Use in Atmospheric Studies, Evaluation No. 17, JPL Publication 10-6, Jet Propulsion Laboratory, Pasadena, 2011.

Schuirmann, D. J.: A comparison of the Two One-Sided Tests Procedure and the Power Approach for assessing the equivalence of average bioavailability, Journal of Pharmacokinetics and Biopharmaceutics, 15, 657–680, doi:10.1007/BF01068419, 1987.

Seinfeld, J. H.: Urban Air Pollution: State of the Science, Science, 243, 745–752, doi:10.1126/science.243.4892.745, 1989.

Shindell, D., Kuylenstierna, J. C. I., Vignati, E., van Dingenen, R., Amann, M., Klimont, Z., Anenberg, S. C., Muller, N., Janssens-Maenhout, G., Raes, F., Schwartz, J., Faluvegi, G., Pozzoli, L., Kupiainen, K., Hoglund-Isaksson, L., Emberson, L., Streets, D., Ramanathan, V., Hicks, K., Oanh, N. T. K., Milly, G., Williams, M., Demkine, V., and Fowler, D.: Simultaneously Mitigating Near-Term Climate Change and Improving Human Health and Food Security, Science, 335, 183–189, doi:10.1126/science.1210026, 2012.

Sillman, S., Logan, J. A., and Wofsy, S. C.: The sensitivity of ozone to nitrogen oxides and hydrocarbons in regional ozone episodes, Journal of Geophysical Research, 95, 1837, doi:10.1029/JD095iD02p01837, 1990.

Singh, H. B., Salas, L., Herlth, D., Kolyer, R., Czech, E., Avery, M., Crawford, J. H., Pierce, R. B., Sachse, G. W., Blake, D. R., Cohen, R. C., Bertram, T. H., Perring, A., Wooldridge, P. J., Dibb, J., Huey, G., Hudman, R. C., Turquety, S., Emmons, L. K., Flocke, F., Tang, Y., Carmichael, G. R., and Horowitz, L. W.: Reactive nitrogen distribution and partitioning in the North American troposphere and lowermost stratosphere, Journal of Geophysical Research, 112, doi:10.1029/2006JD007664, 2007.

Streets, D. G., Bond, T., Carmichael, G. R., Fernandes, S., Fu, Q., He, D., Kilmont, Z., Nelson, S., Tsai, N., Wang, M., Woo, J., and Yarber, K.: An inventory of gaseous and primary aerosol emissions in Asia in the year 2000, Journal of Geophysical Research, 108, doi:10.1029/2002JD003093, 2003.

Streets, D. G., Zhang, Q., Wang, L., He, K., Hao, J., Wu, Y., Tang, Y., and Carmichael, G. R.: Revisiting China's CO emissions after the Transport and Chemical Evolution over the Pacific (TRACE-P) mission: Synthesis of inventories, atmospheric modeling, and observations, Journal of Geophysical Research, 111, doi:10.1029/2006JD007118, 2006.

van der Werf, G. R., Randerson, J. T., Giglio, L., Collatz, G. J., Kasibhatla, P. S., and Arellano, A. F.: Interannual variability

in global biomass burning emissions from 1997 to 2004, Atmospheric Chemistry and Physics, 6, 3423–3441, doi:10.5194/acp-6-3423-2006, 2006.

Vestreng, V. and Klein, H.: Emission data reported to UNECE/EMEP: Quality assurance and trend analysis & Presentation of WebDab, MSC-W Status Rep. 2002, 2002.

Welch, B. L.: The Generalization of Student's problem when several different population variances are involved, Biometrika, 34, 28–35, doi:10.1093/biomet/34.1-2.28, 1947.

West, J. J., Fiore, A. M., Horowitz, L. W., and Mauzerall, D. L.: Global health benefits of mitigating ozone pollution with methane emission controls, Proceedings of the National Academy of Sciences, 103, 3988–3993, doi:10.1073/pnas.0600201103, 2006.

West, J. J., Naik, V., Horowitz, L. W., and Fiore, A. M.: Effect of regional precursor emission controls on long-range ozone transport Part 2: Steady-state changes in ozone air quality and impacts on human mortality, Atmospheric Chemistry and Physics, 9, 6095–6107, doi:10.5194/acp-9-6095-2009, 2009.

Appendix A Total Oxidized Nitrogen Concentrations

The main text shows total oxidized nitrogen partitioning (see Figure 2), but not concentrations of component species [..[359]]NO_x, HNO_3, or PAN. Figure A8 provides concentration data to complement Figure 2.

[359]removed: ,

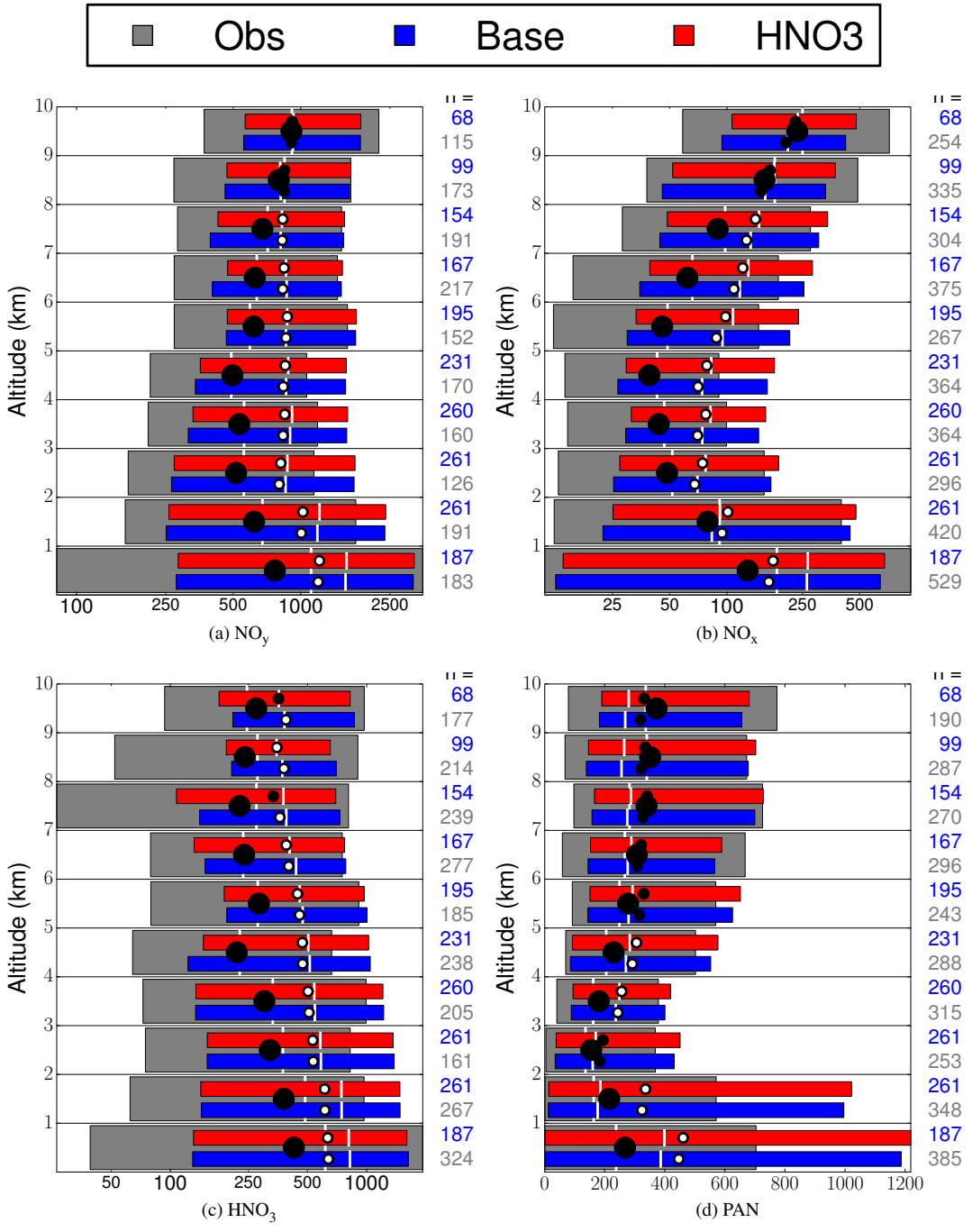

Fig. A8. Same as Figure 2 for concentrations instead of NO_y fractions.

Appendix B Referee Comments and Responses

Each referee comment will be listed and bold. The author comment will follow each referee comment and will be italicized.

Comment: 3220, 21: Instead of speaking of "trade off", simply state "In comparison to regional models, GCTMs have decreased sensitivity to boundary conditions and increased sensitivity to emissions, transport, and chemistry. A reference to some paper showing this comparison would be useful. *Response: Agreed and a reference discussing this comparison has been added.*

Comment: Section 2: In the methods section, the authors need to clarify how they compute an annual forcing, when they only seem to run the GEOS-chem model for the INTEX-A periods. *Response: The portion of the modeling/evaluation related to oxidized nitrogen partitioning was limited by the observation periods; the INTEX-NA Phase-A periods. As such, GEOS-Chem with the updated chemical mechanism was run for that period to develop simulated/observed vertically binned population datasets for analysis. When approaching the radiative effects portion of this study, there were no such limitations. Therefore, a full model year worth of GEOS-Chem output was utilized to determine the annual averaged instantaneous radiative forcing. This clarification will be added to the text.*

Comment: 3225, 14: Is there a reference for P. Wennbergs data? If not, this is fine. *Response: An experiment description for P. Wennbergs data is not provided on the INTEX website. Also, the observation data was retrieved from the INTEX-NA data archive, not from a published paper.*

Comment: 3227, 13: Could the authors be specific as to which techniques are precluded? In addition, is there a reason that a simple r2 regression test would not be valid? *Response: Due to the difference in variance between the two populations, a standard student t-test was precluded. An r2 regression test can be used to compare observed/modeled pairs. However, the method of evaluation used in this study compared observed/modeled vertical bin populations. In addition, the method used in this analysis enabled the display of accepting/rejecting the simulated vs. observed population means as being similar, as shown in Figure 3 (filled/non-filled circles).*

Comment: 3229, 5: "The affect of temper ... altitude." This sentence is misleading. There may be other ways to see the effects. Perhaps the authors choose to evaluate this sensitivity in this manner? *Response: This is the method of evaluation we decided to pursue. The referenced sentences have been updated to the following: For each simulation, we evaluate the model in 1 km vertical bins. This method of evaluation was chosen since temperature, pressure and transport have large variability throughout the vertical troposphere, and these variables play a strong role in the rate of Reaction R1.*

Comment: Section 2.5: Surface radiative forcing is confounded discussion. The authors need to clarify if the forcing is "instantaneous radiative forcing" or "radiative forcing". "Radiative forcing" was defined as the change in flux (at the top of atmosphere or tropopause) including a stratospheric temperature adjustment under the assumption of fixed dynamical heating. If the authors have computed "instantaneous" forcing, then the surface forcing makes sense, otherwise they need to address the extent of atmospheric and surface process adjustments. *Response: The values used in this analysis were based on instantaneous radiative forcing.*

Comment: 3230, 15: While previous papers by Henderson, et. al., have focused on the 8-10 km region,

readers of this paper will be caught off guard by this sentence. Perhaps a note in the introduction, or something clarifying the reason for this focus at this point in the paper would be useful. *Response: An added sentence to provide additional clarification was added to the introduction.*

Comment: In addition, the authors need to clarify whether the radiative forcing is computed as an instantaneous effect, or with the stratospherically adjusted temperature due to fixed dynamical heating. If Strat. Adjust. was not used, then the 4 month equilibrium is a red herring. *Response: The radiative effects were calculated as an instantaneous radiative forcing and all values relating to the radiative effects analysis were reported as annual average instantaneous radiative forcing in mW/m^2. Updates to the manuscript have been made to make this clearer. As well, the 4-month equilibrium was eliminated and the calculations were re-run. The annual average instantaneous radiative forcing values changed by ¡ 0.1 mW/m^2. The values have been updated.*

Comment: One more clarification would be to state that the "change in flux" is a net increase in net downward solar and terrestrial flux due to the change in mechanism. (both "net"s are necessary as well as the "downward") You could, instead, simply refer to net trapped energy. *Response: The radiative flux, which is how results in this analysis are presented, is defined as the net increase in net downward solar and terrestrial (combined) radiation. This sentence has been added in the radiative effects methods section to provide clarification.*

Comment: 3235, 3: "Due to the increase... " "The increased ozone leads to a net increase in trapped energy beneath the top of the atmosphere of ... and beneath the atmosphere of... Please also clarify that for the sulfate aerosol, the increase the albedo of the earth system, reflecting additional solar radiation to space. *Response: These sentences were updated to the following: The increase in ozone caused an increase in instantaneous radiative forcing at the surface and the top of the model of 10.4 mW/m^2 and 31.1 mW/m^2, respectively. Similar to ozone, there was a net increase in sulfate aerosols, which occurred mainly in the lower troposphere and over landmasses. These increases resulted in a net decrease in instantaneous radiative forcing, driven by the reflectance of incoming solar radiation. The decreases were -3.3 mW/m^2 and -3.0 mW/m^2 at the surface and top of the model, respectively.*

Comment: 3235, 10-20: I am uncertain what the authors are trying to say. This paragraph needs to be rewritten. Perhaps they are trying to say that while the methods and altitude at which radiative forcing are computed are different from those used in the IPCC, the relative magnitude of the correction indicated that the change to the kinetics could be important to understanding processes relevant to policy? If so, this paragraph may belong in the conclusion rather than results. *Response: This paragraph was re-written to provide clarification and moved to the discussion portion of the paper.*

Comment: 3235, 26: "Also, a larger magnitude of forcing.... surface. The net atmos..... precipitation. Perhaps the authors mean "The net absorption of energy by the atmosphere as seen in the third panel of figure 4 will affect convective and transport processes." While the reference to Shindells analysis is nice, does the total of the ozone effect and the aerosol effect lead to a clear effect on precipitation that is explicitly confirmed by the results in this paper, or should this also be in the discussion? *Response: Those sentences were poorly constructed. The updated sentence in the results section defines net atmospheric forcing, as defined by Shindell. The portions related to the significance of atmospheric forcing have been relocated to the discussion.*

Comment: 3236, 5: Do the authors mean "indirect effects" or "atmospheric responses and feedbacks"? *Response: First, this sentence was moved from the results to the discussion. Second, atmospheric responses and feedbacks is the better description.*

Comment: 3236, 5: Do the authors mean "simulation" or "offline computation"? *Response: Offline computation.*

Comment: 3236, 7: Are the "localized adjustments" an increase or decrease in oxidation of the SO2 to SO4? And is there data to back up this assertion? *Response: The adjustments led to an increase in the oxidation of SO2. The sentence was updated to the following: This increase in OH-1 enables an increase in the oxidation of SO2 to SO4. This was inferred based on the decrease in the reaction rate of R1, which increases OH-1.*

Comment: 3236, 23: both HNO3 and NOx have an inverse relationship with what? Perhaps with each other? Would a scatter plot make that inverse relationship clear? *Response: For the purposes of this assessment, where the only change in the GCTM was an update to R1, HNO3 and NOx are expected to have an inverse relationship with each other. I believe a reference to R1 within the text around this area should suffice and a scatter plot is not required.*

Comment: 3236, 25: Why are these counterintuitive? Is there a reason for these to be opposite our intuition? It would be useful to have a reason why these results are the opposite of the direct effect of the kinetics. *Response: The decrease in the reaction rate of R1 would lead one to believe that NOx would increase and HNO3 would decrease. However, the opposite was seen at the surface. When reviewing the vertical spatial profiles of these two species, it is seen that this only occurred at the surface and the rest of the troposphere produced changes in NOx and HNO3 concentrations in patterns that would be expected due to the decrease in R1s reaction rate. The reasoning will be further explored in the coming weeks while the re-write is being completed.*

Comment: 3237, 10: "The previous hypothesis"... I do not know to which hypothesis the authors refer. Perhaps the discussion of sulfate distribution belongs in another paragraph stating that the sulfate concentrations are more localized to the surface and to more polluted areas. *Response: This was a poorly constructed sentence. The sentence was updated to the following: For sulfate, Fig. 8 indicates that the surficial changes occurred in the same localized regions as the concentration changes to HNO3 and NOx.*

Comment: 3237, 19: I do not know what is meant by "Literature updates". Perhaps "Updates to the NO2+HO reaction rate provided by () have been implemented in GEOS-Chem. The resulting changes in chemistry composition more closely match the INTEX observations. In particular we find..." *Response: Clarifications were made and the two sentences were updated to the following:Updates to the NO2 + HO-1 reaction rate, as suggested by Mollner (2010) and Henderson (2012), have been implemented in GEOS-Chem. The resulting model performance was evaluated using observations from the INTEX-A campaign.*

Comment: 3238, 1 I dont know what is meant by "was decreases". Perhaps the authors mean to say, "Decreases in Nox lead to a near global increase in ozone. The resulting increase in oxidation potential leads to an increase in sulfate. Additional work needs to be done to understand the surface layer concentrations of HNO3 and NOx, as they are contrary to the direct implication of the decreased reaction rate coefficient." *Response: That more clearly states what was intended. As well, it was moved to a more appropriate place in the*

discussion. That particular sentence was simplified and rewritten.

Comment: 3238, 18: The authors need to clarify what they mean by "performance". *Response: This is acknowledged and further clarification will be included in the re-write.*

Comment: 3238, 28: "change in ozone sensitivity". Sensitivity to what? *Response: Sensitivity was a poor choice of words. Rather Similar to the changes in oxidized nitrogen concentrations, the change in simulated ozone concentrations is modest.*

Comment: Paragraph starting at 3238, 28: This paragraph needs help. I dont know what is meant by "modest", or how a "model uses NOx". Do the authors mean "sensitivity of predicted O3" or "change in O3 concentrations"? I am having a hard time understand the specific meaning of these sentences. *Response: This paragraph will be revised in the re-write.*

Comment: Paragraph starting at 3239, 9: The first two lines of this paragraph could be rewritten to say, "The radiative effects of the change in ozone and sulfate distributions was evaluated with an offline radiative transfer code". Please refer to previous discussion of how to be precise about forcing numbers. (Yes, I know this is a bother. Thanks for being precise.) Do you mean variance or change? *Response: The forcing numbers were the results of annual average instantaneous radiative forcing. The sentence was changed to the following: The radiative effects due to the changes in ozone and sulfate concentrations were evaluated using an offline radiative transfer model. Also, this is not a bother. Being precise is important.*

Comment: 3239, 25: To which policy implications do the authors refer? I do not understand the second sentence of this paragraph. Do the authors mean "robust" or "very similar"? Why do the updates need lab confirmation? What additional evidence, in particular, would be helpful? *Response: References to policy implications relate to surficial pollutant concentrations and emissions. While the mechanism largely improved oxidized nitrogen partitioning, the changes in trace gas concentrations that we analyzed were not significant enough to alter either of these policy drivers. Overall, this final paragraph was mostly rewritten.*

Comment: For all figures: Are these annual averages, or only average during the INTEX period. *Response: They actually vary and updates to specify which is used have been added to each necessary figure description.*

Comment: 3232, 29: In addition, is there a reference for the fact that the baseline model has a high bias? *Response: The high bias in the model that is being referenced is based on the results from the baseline model and the INTEX-A observations.*

Comment: The chemical reaction examined here critically influences NOy and HOx chemistry and compounds oxidized by HO. Thus, it should be noted that changing this reaction rate may affect other aspects of model performance not examined here, and the potential shortcomings of adjusting one reaction rate in isolation. *Response: This was considered in Henderson et al. (2012; doi: 10.5194/acp-12-653-2012), where the magnitude of the updated mechanism used in this study was developed. A detailed explanation of these other considerations was detailed in that publication. However, this is a very important point and should certainly be reiterated in this paper. I will make sure a discussion regarding this topic is included at some point in the introduction.*

Comment: It would be helpful to compare the new reaction rate with the rate assumed in the base case

as a function of temperature, and to more clearly note which study is used in the base case (p. 3224). *Response: The base case used in this study is the out-of-the-box version of the GEOS-Chem model. And I agree it is useful to visualize the different reaction rates. This can be seen in Figure 5 of Henderson et al. (2012; doi: 10.5194/acp-12-653-2012).*

Comment: What is the basis for determining that CH3O2NO2 was estimated within a factor of two (p. 3225, lines 27-29)? Also, it is unclear what is referred to by the GEOS-Chem levels of 15 ppt are 34 ppt (p. 3226, line 2) are these medians in each layer? *Response: Clarifications can and will be made to this paragraph. The factor of two for MPN is the difference between the estimated concentrations of MPN from the discussed chemical box-model and GEOS-Chem results from an updated version that includes MPN. The results from each model are the median values and this has been added to the text for clarity.*

Comment: How were duplicates removed (p. 3229, line 15)? Was an average of the observations kept for the corresponding model prediction? *Response: Removed is probably the wrong way to view this model/observation population formation and a re-phrasing would help. Rather, the model results werent double counted. If the observations produced X number of values that would all correspond to a particular grid cell in a particular temporal period (one 4-D modeled point), the modeled population pool would not be diluted with X number of repeated values.*

Comment: What is the basis for concluding that lightning NOx is the reason for the high bias in NOy? *Response: The certainty with which that was stated on p. 3231, line 25 should be more along the lines of a hypothesis; and probably moved to the discussion. This study did not focus on lightning produced NOx and as such, should probably not reach such sweeping conclusions. Nonetheless, this is hypothesized for the following reasons: Sources of NOx in the upper troposphere include convectively lofted anthropogenic NOx, lightning, transport from the stratosphere and aircraft emissions (Jaegle 1998, Hudman 2007). The observations are filtered to exclude stratospheric intrusion and Allen et al. (2012) found that the impact of aircraft NO emissions on upper tropospheric NOx on a flight path from the INTEX-A campaign were generally small. Though, it was stated that the impacts related to aircraft NO emissions are more evident in periods of low lightning NO emissions. This leaves either lightning NOx or convectively lofted anthropogenic NOx as the main culprits. Hudman et al. (2007) studied upper tropospheric NOx during the INTEX-A campaign using GEOS-Chem and found that lightning was the dominant factor in upper tropospheric NOx bias. Though, their main bias was in regions of the upper troposphere above the domain of interest for this study and was low biased. As well, their version of GEOS-Chem utilized an older vertical release profile of lightning NOx. Newer GEOS-Chem versions, such as the one used in this study, utilize the vertical release profiles developed by Ott et al., (2010). In these updated profiles, large portions of upper and lower tropospheric lightning NOx fractions were moved to the middle troposphere. These areas happen to be the areas where the high bias of NOx/NOy partitioning and NOx concentrations mainly occur. Therefore, it was hypothesized that these biases were a result of the vertical lightning NOx release profiles. This will be added to the discussion, as well.*

Comment: It is unclear whether significant improvements have in fact been demonstrated by the evaluations against aircraft data. Both cases had substantial biases for concentrations, leading to the use of the fractional approach. In most cases, the changes in the modeled fractions were small relative to the gaps

between model and observations. It was also difficult to view these differences in Figure 3, as the white lines in the grey bars are barely visible, and the meaning of the large circles is not explained. The justification for focusing on results above 8 km was also unclear. In sum, more caution is warranted in the conclusions, especially given the shortcomings of the emissions inventory and the possibility of other errors in the chemical mechanism. *Response: The large circles are the mean values for the observation population in each vertical bin. This description will be added to the Figure description. The reason why this evaluation focused mainly on the upper troposphere is because Henderson et al. (2012; doi: 10.5194/acp-12-653-2012) targeted the upper troposphere when updating the chemical mechanism. Also, the changes between the base case and the HNO3 case are strongest in the upper troposphere, where temperatures are lowest. Nonetheless, the evaluation in this analysis spanned most of the troposphere. Regarding significant improvements, I agree with your assessment on the use of such words, though approached from a different viewpoint. In model evaluations, the use of statistics is paramount and in statistics, the word significant generally has a specific definition. In this evaluation, partitioned oxidized nitrogen species and oxidized nitrogen species concentrations did improve in statistically significant manners for a few vertical profile bins through the use of the updated mechanism; but, it is certainly limited. However, there are still some instances of significant model bias, as you pointed out. On an overall basis, the updated chemical mechanism did provide, at least, incremental improvements in the model; and that has value.*

Comment: Given the fractional approach, PAN does not provide unique information. Also, NOx and HNO3 are more clearly affected by this reaction rate than PAN. A more direct evaluation might be obtained by considering the ratio (NOx/HNO3), rather than the three fractional components. *Response: I agree that NOx and HNO3 are more clearly affected by this reaction rate than PAN. However, PAN is a significant portion of NOy and is affected by the update (as mentioned in the discussion). Regarding the NOx/HNO3 ratio, that value was utilized in the development of the HNO3 chemistry used in this analysis.*

Comment: I encourage the authors to find a different name for their sensitivity case than HNO3 case, which is unclear and becomes cumbersome given the numerous comparisons of HNO3 levels. *Response: This point is noted and will be considered.*

Comment: Why werent the radiation comparisons evaluated at the tropopause? *Response: The version of PORT that was used in the assessment only computed the radiative flux at the surface and the top of the model. Since the ACPD publication, Ive compiled a newer version with tropopause data included. Therefore, that can be added, if recommended.*

Comment: Though its noted that the increase in HNO3 and decrease in NOx are counter intuitive and limited to the surface (Figure 6), this surprising result warrants further investigation and explanation. *Response: Upon revisitation of the text, I do agree that this result warrants further investigation and discussion. The reasoning will be further explored in the coming weeks while the re-write is being completed.*

Comment: A high-bias is noted for HO (p. 3238); does reducing the reaction rate exacerbate that change? *Response: Yes, and this loops back to the thoughts in the comment above. Decreasing the formation of nitric acid certainly increases the availability of NOx and OH. However, this radical will then adjust other atmospheric chemistry process (ex. sulfate), rather than creating a 1:1 ratio increase in OH concentrations.*

Comment: Figure 2: The VHF and SADS profiles are not explained in the text *Response: That omission*

will be corrected in the write-up.